ADVANCED HEALTHCARE MATERIALS
www.advhealthmat.de

Cell-Derived Vesicles with Increased Stability and On-Demand Functionality by Equipping Their Membrane with a Cross-Linkable Copolymer

*Xinan Huang, Dimitri Hürlimann, Hendrik T. Spanke, Dalin Wu, Michal Skowicki, Ionel Adrian Dinu, Eric R. Dufresne, and Cornelia G. Palivan**

Cell-derived vesicles retain the cytoplasm and much of the native cell membrane composition. Therefore, they are attractive for investigations of membrane biophysics, drug delivery systems, and complex molecular factories. However, their fragility and aggregation limit their applications. Here, the mechanical properties and stability of giant plasma membrane vesicles (GPMVs) are enhanced by decorating them with a specifically designed diblock copolymer, cholesteryl-poly[2-aminoethyl methacrylate-*b*-poly(ethylene glycol) methyl ether acrylate]. When cross-linked, this polymer brush enhances the stability of the GPMVs. Furthermore, the pH-responsiveness of the copolymer layer allows for a controlled cargo loading/release, which may enable various bioapplications. Importantly, the cross-linked-copolymer GPMVs are not cytotoxic and preserve in vitro membrane integrity and functionality. This effective strategy to equip the cell-derived vesicles with stimuli-responsive cross-linkable copolymers is expected to open a new route to the stabilization of natural membrane systems and overcome barriers to biomedical applications.

1. Introduction

The inherent complexity of biological membranes and compartments has inspired the development of a variety of simplified model systems with tailored structures, components, and specialized functions.[1] Various synthetic or purified lipids have been used for the formation of vesicular architectures such as liposomes or giant unilamellar vesicles (GUVs), whose membrane mimics the cell membrane in terms of permeability, fluidity, and dynamic behavior.[2–8] However, there are major limitations of lipid-based vesicles (liposomes, GUVs), including the lack of the complex composition of cell cytosol, the lack of the protein density and lipid diversity of the living cell membranes, and the difficulty in reconstitution of properly oriented multiple transmembrane proteins.[9,10] In addition, as lipid-based vesicles cannot be created with similar lipid diversity and protein density as the membrane of living cells, a particularly appealing alternative is the production of natural cell-derived vesicles, such as extracellular vesicles (EVs) and giant plasma membrane vesicles (GPMVs). Cell-derived vesicles inherit from the donor cells the cytoplasm (without internal organelles) and the cell membrane, which embeds to a significant extent the naturally occurring proteins, lipids, and glycocalyx.[11–16] The advantage of being close-to-nature makes cell-derived vesicles more appealing for complex applications than artificial lipid-based vesicles. Extracellular vesicles with nanometer sizes obtained from prokaryotic and eukaryotic cells retain—inside their cavity—DNA, RNA, and proteins.[17,18] Therefore, they are good candidates for biological applications, e.g., as diagnostic biomarkers of prostate,[11,19] lung,[20] breast,[21] colorectal,[22] ovarian,[23] and pancreatic cancer.[24] Additionally, EVs have been also intensely investigated as delivery vehicles for therapeutic agents, such as miRNA,[25] siRNA,[26,27] tumor antigenic peptides,[28,29] doxorubicin,[30,31] and paclitaxel.[32] However, their use in biomedical applications is still limited because of difficulties in production (e.g., isolation and purification)[33,34] and poor stability.[35–38] On the contrary, GPMVs, which are micrometer-size vesicles, can be easily produced and purified from intact living donor cells[39–41] and then analyzed by direct

X. Huang, D. Hürlimann, D. Wu, M. Skowicki, I. A. Dinu, C. G. Palivan
Department of Chemistry
University of Basel
BPR1096, Mattenstrasse 24a, Basel 4058, Switzerland
E-mail: cornelia.palivan@unibas.ch
D. Hürlimann, M. Skowicki, I. A. Dinu, C. G. Palivan
NCCR-Molecular Systems Engineering
BPR1095, Mattenstrasse 24a, Basel 4058, Switzerland
H. T. Spanke, E. R. Dufresne
Laboratory for Soft and Living Materials
Department of Materials
ETH Zurich
Vladimir-Prelog-Weg 5, Zurich 8093, Switzerland

The ORCID identification number(s) for the author(s) of this article can be found under https://doi.org/10.1002/adhm.202202100

DOI: 10.1002/adhm.202202100

microscope visualization.[42] GPMVs are most commonly generated by chemically induced blebbing of the cell plasma membrane using vesiculation solution containing N-ethylmaleimide (NEM)[43] or dithiothreitol (DTT)/paraformaldehyde (PFA).[44] Less conventional approaches are based on the chloride salt solution treatment[41] and laser irradiation of the cells.[45] GPMVs have been frequently used as a model system to investigate membrane properties, such as reversible addition–fragmentation chain transfer-associated phenomena,[43,46] membrane penetration of amphiphilic quantum dots,[47] and viral membrane fusion.[48] Recently, GPMVs have been reported for the first time to serve as artificial cells by internally equipping them with nanometer-sized artificial organelles, which retained their integrity and functionality in vivo, in a zebrafish model.[49] However, their membrane, similarly to that of EVs, has a lower stability and therefore disruption might occur over time under physiological conditions, limiting their long-term in vivo applications.[50]

The most common approach to increase the stability of lipid-based vesicles (liposomes, GUVs) is to incorporate various hydrophilic polymers (e.g., polyethylene glycol), as steric stabilizers within the lipid bilayer either by covalent bonding to the head group of lipids (PEGylation) or by adsorption onto the outer surface.[51–56] Although effective in the case of simple synthetic lipid membranes, this concept is incompatible for stabilization of cell-derived vesicles. To date, the modification of EVs surface has been only focused on tuning their chemical and biological behavior. For example, cholesterol was inserted in their membrane to change its fluidity and rigidity,[57] proteins were grafted on EVs surface to provide functionality,[58] and nucleic acids were attached for targeted delivery.[59] Nevertheless, their bioapplication range is drastically narrowed down by the poor membrane stability and disruption in biological environments.[36,37] To broaden their usage in biomedical applications, a key requirement is to improving the EVs stability.[35,60] Thus, the use of polymers to strengthen the membrane of cell-derived vesicles is a concept that still needs to be explored. In a few very recent findings, the surface of EVs was modified with DNA, considered as a linker to attach polymers,[38] or by sequential deposition of a polyelectrolyte multilayer.[61] While the DNA tethering method to attach polymers at the surface of EVs is effective as a model to stabilize their membrane in solution,[38] the risk of polymer detachment in vitro, due to DNA cleavage by DNases, has still to be overcome. On the other hand, slight changes in the delicate balance of electrostatic interactions governing the layer-by-layer deposition of a polyelectrolyte multilayer on the exterior of the EVs membrane might induce the disassembly of the multilayer and the rupture of the EVs membrane. For bioapplication of cell-derived vesicles, the development of approaches to stabilize their membranes over prolonged timeframes (i.e., days) is of a key importance. In addition, there are no reports implementing EVs with emerging properties, as for example stimuli-responsiveness, which are essential for biomedical applications.

We present here a strategy to improve the stability of vesicles derived from living cells, by insertion of a specifically designed block copolymer in their membrane and subsequent cross-linking without affecting the architecture or composition of the vesicles. We chose GPMVs since they preserve the lipid composition and a variety of membrane proteins of the intact plasma cell membranes together with the cytoplasm of the donor cells (except organelles). In addition, they have been reported to allow being loaded with desired molecules and nanoobjects prior up taken by the donor cells.[49] The membrane of GPMVs contains a variety of membrane proteins, receptors, etc., that are inducing more complex conditions and interactions, eventually resulting in a completely different stability and flexibility compared to a simple liposome membrane. First, we synthesized a cholesteryl-poly[2-aminoethyl methacrylate-*b*-poly(ethylene glycol) methyl ether acrylate] (Chol-PAEMA-*b*-PEGMA) diblock copolymer, which displays three domains, each with a specific function: i) a hydrophobic cholesteryl moiety serving as an anchor to be inserted into the vesicles membrane, ii) a hydrophilic PAEMA block providing a plethora of pendant amino groups as cross-linking sites to form the stable, external polymer shell on the surfaces of vesicles, and iii) a PEGMA block to improve the biocompatibility (**Figure 1**). The second step was to generate GPMVs from the donor cells by cell-treatment with a vesiculation solution followed by their isolation.[39] GPMVs were then combined with different amounts of Chol-PAEMA-*b*-PEGMA under mild conditions, aiming to obtain copolymer-supplemented GPMVs with a hybrid membrane based on the cell membrane with inserted diblock copolymers. Finally, the copolymer has been cross-linked to increase the mechanical stability of GPMVs.

The stability of the cross-linked-copolymer GPMVs was evaluated by surfactant resistance and dye permeation studies using confocal laser scanning microscopy (CLSM). Vesicle fluctuation analysis served to determine the bending rigidity of cross-linked-copolymer GPMVs and evaluate the membrane mechanical stability against bending deformations. To further advance their application, we investigated their stability over time under specific storage conditions and evaluated their toxicity in a HeLa cell line. Moreover, we extended the strategy for two other cell lines to prove the versatility of our approach. We expect the excess of amine groups in the PAEMA block to allow for protonation and swelling of the polymer layer in slightly acidic conditions (pH 6.0–6.5). We have thus studied the effect of pH changes on the diffusion of molecules into and out of the cross-linked-copolymer GPMVs to evaluate their potential for application in biosensing and drug delivery. In addition, we explored the accessibility of membrane biomolecules after GPMVs modification by immunofluorescent staining of the membrane receptors. Our study introduces cell-derived vesicles endowed with an improved stability and "on-demand" functionality. Such hybrid biomaterials benefit from the combination of a cell-derived compartment with a synthetic polymer tailored both to solve the issue of reduced membrane stability and to induce emerging properties such as stimuli-responsiveness. We believe that our work opens new avenues for obtaining stable biomembranes with stimuli-triggered permeability, highly in need for biological applications.

2. Results and Discussion

2.1. Synthesis and Characterization of Chol-PAEMA-*b*-PEGMA Diblock Copolymer

Physical cross-linking (hydrogen bonding or electrostatic interactions) of liposome membranes with cholesteryl-conjugated polymers has been previously employed for a short-term

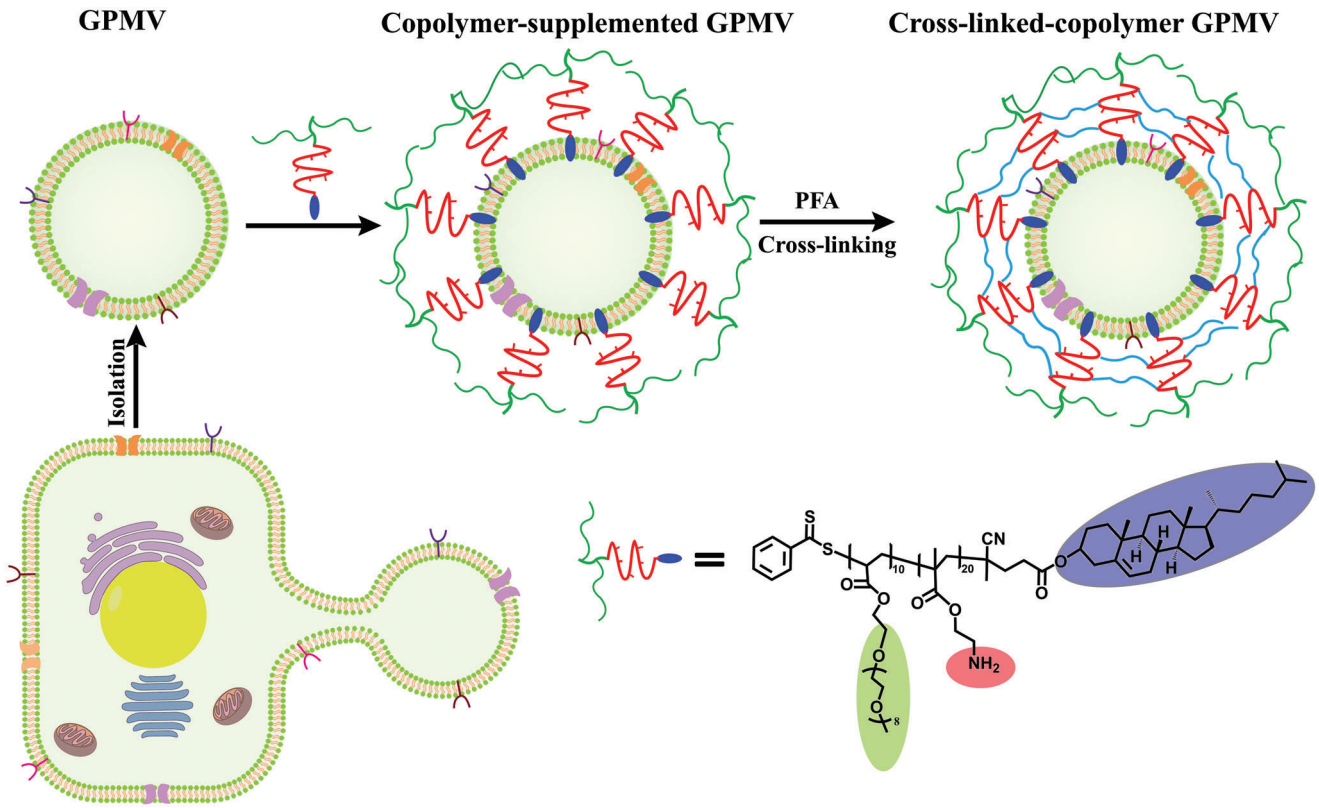

Figure 1. Schematic representation for preparation of cross-linked-copolymer GPMVs. First, GPMVs are generated and isolated from cells (left), then the Chol-PAEMA-*b*-PEGMA diblock copolymer is inserted into the GPMVs membrane (middle) and finally, the cross-linked polymer shell is formed around GPMVs (right).

stabilization of lipid membranes.[62,63] By contrast, we propose here a covalent cross-linking approach to preserve the architecture and composition of cell-derived vesicles over prolonged timeframes (i.e., days). As the cross-links formed by covalent bonds between polymer chains are stronger than physical intermolecular interactions,[64,65] this approach has been selected to combine the nature-derived GPMV membrane with a cross-linkable copolymer to render the membrane more mechanically stable. To this end, we designed a water-soluble diblock copolymer, Chol-PAEMA-*b*-PEGMA, that can be easily inserted in the membrane of GPMVs due to the cholesteryl anchoring moieties.[49,66] In addition, the amine groups of PAEMA block allow for cross-linking, whereas the PEGMA block serves as hydrophilic domain to improve the biocompatibility of the copolymer shell.[67] As not all amine groups from the PAEMA blocks are involved in the cross-linking procedure, their exposure to acidic conditions will induce polymer swelling and stretching due to the charge repulsion between the protonated amine groups. Chol-PAEMA-*b*-PEGMA copolymer was synthesized starting from a cholesteryl-terminated RAFT agent via RAFT polymerization (**Figure 2**), which allows the facile cholesteryl end functionalization of the polymer chains.[68] Synthesis of cholesteryl-terminated RAFT agent was achieved via Steglich esterification of the cholesterol hydroxyl group with 4-cyano-4-(phenylcarbonothioylthio)pentanoic acid (CPDB) in the presence of *N*,*N*′-dicyclohexylcarbodiimide (DCC) as coupling agent and 4-(dimethylamino)pyridine (DMAP) as catalyst.[69] The successful synthesis of cholesteryl-terminated RAFT agent was established by ^{1}H nuclear magnetic resonance (^{1}H NMR) spectroscopy (Figure S1, Supporting Information). The proton signals in the 7.3–8.0 ppm range were assigned to the aromatic protons of CPDB, whereas the signal at δ = 3.53 ppm, corresponding to the indicated protons of cholesterol (Figure S1A, Supporting Information), was shifted to δ = 4.64 ppm in the ^{1}H NMR spectrum of cholesteryl-terminated RAFT agent (Figure S1C, Supporting Information), after the reaction with CPDB.[70,71]

Cholesteryl-terminated RAFT agent was then used as a chain transfer agent (CTA) to polymerize the Boc-protected aminoethyl methacrylate monomer (BocAEMA). The chemical structure of Chol-PBocAEMA$_{20}$ was established by the appearance in the ^{1}H NMR spectrum of a proton signal at δ = 1.4 ppm assigned to the Boc-protective group (Figure S2A, Supporting Information). The number average molecular weight (M_n) of 5676 g mol^{-1} and a narrow dispersity ($Đ$) of 1.14 were determined for Chol-PBocAEMA$_{20}$ by gel permeation chromatography (GPC) (Figure S3, Supporting Information). The polymerization of EGMA was performed using Chol-PBocAEMA$_{20}$ as a macroinitiator. The chain extension of the PEGMA block was followed by ^{1}H NMR spectroscopy, where the peak at δ = 3.6 ppm was attributed to the O–CH_2–CH_2 protons (Figure S2B, Supporting Information). After the formation of the second block, the GPC trace (Figure S3, Supporting Information) shifted to a higher molecular weight (M_n = 9211 g mol^{-1}, $Đ$ of 1.35), which also indicates a

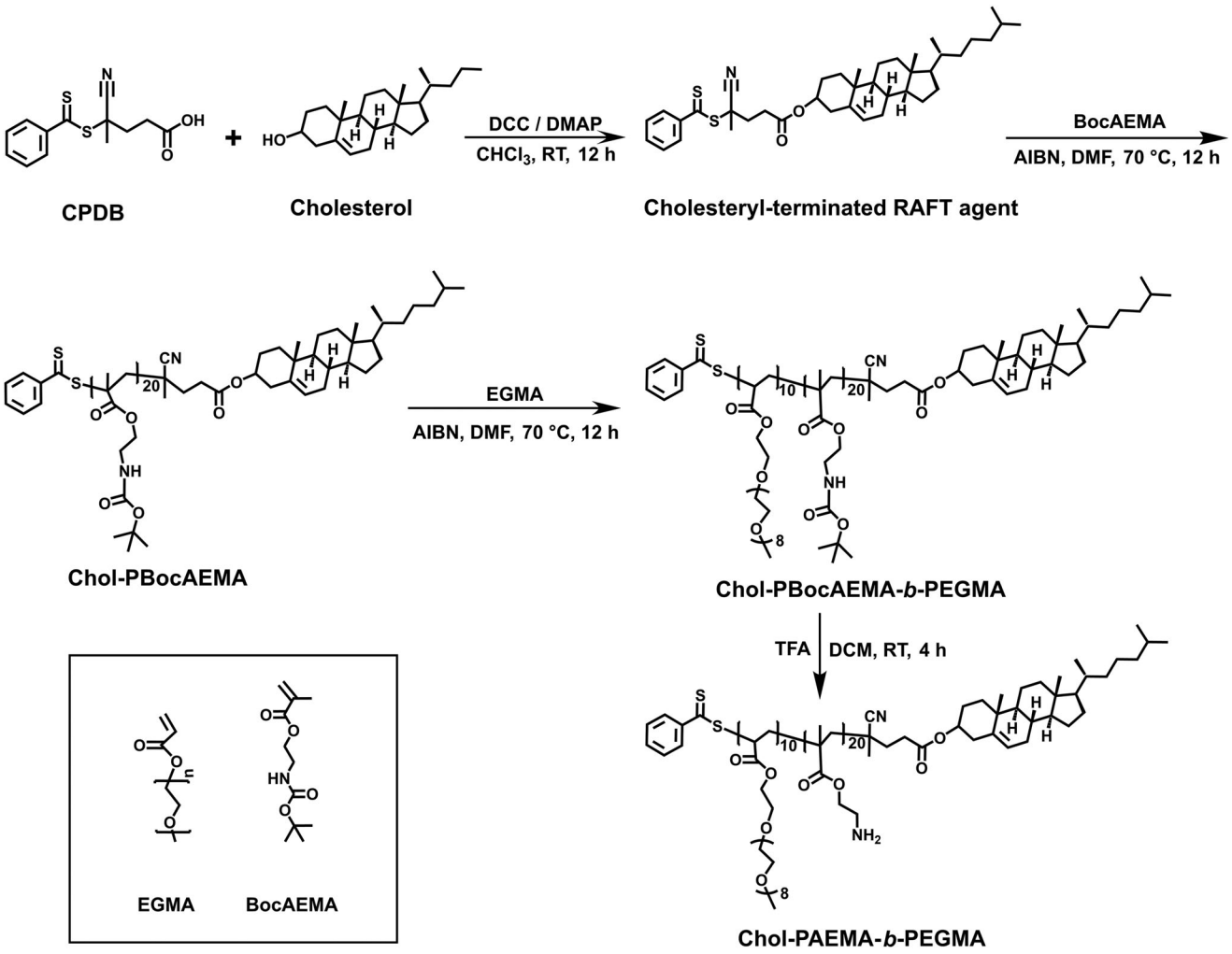

Figure 2. Synthesis of Chol-PAEMA-*b*-PEGMA diblock copolymer via sequential RAFT polymerization of BocAEMA and EGMA monomers, starting from a cholesteryl-terminated RAFT agent.

successful synthesis of Chol-PBocAEMA$_{20}$-*b*-PEGMA$_{10}$. Finally, Boc protective groups were removed by treatment with trifluoroacetic acid (TFA) to yield Chol-PAEMA$_{20}$-*b*-PEGMA$_{10}$ containing free amines.[72] After deprotection, the signal at $\delta = 1.4$ ppm assigned to the methyl protons of Boc groups completely disappeared in the ^{1}H NMR spectrum of Chol-PAEMA$_{20}$-*b*-PEGMA$_{10}$ (Figure S2C, Supporting Information). Besides this, a PAEMA-*b*-PEGMA diblock copolymer was also synthesized to allow the comparison between the cholesteryl-terminated copolymer and the cholesterol-lacking copolymer (Figure S4, Supporting Information). The polymerization of PBocAEMA$_{19}$ was conducted using CPDB as a CTA, and the analysis by ^{1}H NMR spectroscopy revealed the presence of the peak at $\delta = 1.4$ ppm, corresponding to the Boc protecting groups (Figure S5A, Supporting Information). The further chain extension with PEGMA yield to the diblock copolymer, when the appearance of a strong peak at $\delta = 3.6$ ppm in the ^{1}H NMR spectrum proved the addition of PEGMA block (Figure S5B, Supporting Information). After deprotection, the chemical structure of final PAEMA$_{19}$-*b*-PEGMA$_7$ diblock copolymer was confirmed by the disappearance from the ^{1}H NMR spectrum of the proton signal ($\delta = 1.4$ ppm) assigned to the Boc groups (Figure S5C, Supporting Information).

2.2. Modification of the GPMV Membrane by Insertion and Cross-Linking of the Diblock Copolymer

The formation of cross-linked-copolymer GPMVs involves three steps (Figure 1). First, we generated GPMVs by treating HepG2 cells with vesiculation solution containing DTT and PFA. After 2 h, homogeneous vesicles with a size ranging from 5 to 14 μm were obtained and collected by centrifugation. In the second step, a low amount of dye (Atto-488-NHS-ester) has been added to the Chol-PAEMA-*b*-PEGMA copolymer (initial molar fraction of 0.41%) to label a minor fraction of the polymer chains and to preserve the free amine groups for cross-linking after insertion in the membrane of GPMVs. The dye labeling efficiency was calculated to be 54% and the final molar fraction of labeled polymer chains was 0.22%. The mixture of labeled and unlabeled polymer chains was added in increasing concentrations (0.1, 0.2,

0.25 mg mL^{-1}) to a solution of GPMVs in GPMV buffer (10 mM HEPES, 150 mM NaCl, 2 mM $CaCl_2$, pH 7.4). After 20 min, the Atto-488 labeled copolymer-supplemented GPMVs were washed with GPMV buffer and the insertion of copolymer into the membrane of GPMVs was evaluated by CLSM (**Figure 3**).

In order to establish whether cholesterol is responsible for the insertion of copolymer into the GPMV membrane, we investigated by CLSM the interaction of GPMV membrane with Atto-488 labeled PAEMA-*b*-PEGMA and Chol-PEG5000-FITC, respectively (Figures S6 and S7, Supporting Information). The low fluorescence signal detected when Atto-488 labeled PAEMA-*b*-PEGMA was added to GPMVs (Figure S6, Supporting Information) indicates no insertion and a weak interaction with the GPMV membrane. On the contrary, the bright fluorescent ring observed when Chol-PEG5000-FITC was added to GPMVs, clearly shows that cholesteryl moieties served as anchoring groups for the insertion of diblock copolymer into the GPMV membrane (Figure S7, Supporting Information).[49] The heterogeneous fluorescence intensity of the GPMVs membrane after the insertion of the copolymer (Figure 3B,D) can be explained by the variable composition of the GPMV membrane in terms of lipid diversity and protein distribution.[43] In addition, the increase of the cholesterol content in the GPMV membrane can induce lipid phase separation and formation of more liquid-ordered phase fractions,[73] which will determine a heterogeneous distribution of the inserted copolymer. In the third step, the copolymer-supplemented GPMVs were treated with a PFA solution in GPMV buffer at room temperature (RT), resulting in cross-linked-copolymer GPMVs. The cross-linking effect was assessed by addition of PFA to a solution of Chol-PAEMA-*b*-PEGMA dissolved in GPMV buffer. The copolymer solution became turbid (Figure S8, inset image, Supporting Information). The average hydrodynamic diameter (D_H) of 30 ± 8 nm determined by dynamic light scattering for the cross-linked Chol-PAEMA-*b*-PEGMA was substantially larger than the D_H of the polymer chains before cross-linking, in solution (4 ± 1 nm), which indicated the successful cross-linking of copolymer (Figure S8, Supporting Information).

To optimize the concentration of the diblock copolymer used for insertion into the GPMV membrane, three different copolymer concentrations (0.1, 0.2, 0.25 mg mL^{-1}) were evaluated after the copolymer anchoring and its subsequent cross-linking (Figure 3). Both copolymer-supplemented GPMVs and cross-linked-copolymer GPMVs preserved the membrane morphology at lower copolymer concentration (0.1 and 0.2 mg mL^{-1}). When the copolymer concentration increased to 0.25 mg mL^{-1}, the GPMV membrane was deformed into an irregular shape (Figure 3C, right panel). It is apparent that the membrane deformation is caused by an increase in the surface area of the external leaflet (upper side of the bilayer) when the copolymer concentration is too high (Figure 3A–C, images on the right side), which is in agreement with other reports on protein penetration into a bilayer membrane.[74,75] The incorporation of an amphipathic protein helix into the interfacial section of a bilayer induces membrane deformation due to the bilayer surface-area discrepancy.[74,75] As consequence, 0.2 mg mL^{-1} represents the optimum copolymer concentration that counterbalanced the copolymer density required for the cross-linking reaction with the preservation of GPMVs membrane morphology. Therefore, this copolymer concentration has been applied for stabilization of the membrane of GPMVs.

To quantify the content of copolymer chains inserted into the GPMV membrane, we used the fluorescence intensity of the labeled-Chol-PAEMA-*b*-PEGMA fraction inserted into the GPMV membrane. After insertion, we solubilized the copolymer-supplemented GPMVs by the addition of sodium cholate hydrate (50 μM) and measured the fluorescence intensity of the solution. We calculated the total number of copolymer chains per unit of surface area based on the molar fraction of labeled polymer chains and the initial concentrations of the copolymer mixture: 0.1, 0.2, and 0.25 mg mL^{-1} (Figure S9 and Table S1, Supporting Information). The values of the polymer density inside GPMV membranes of 0.13 ± 0.01, 0.21 ± 0.02, and 0.32 ± 0.02 copolymer chains per nm^2 are significantly smaller than the density of lipid molecules within a cell membrane (about 5 lipid molecules per nm^2).[76] The polymer chains density inside the GPMV membranes is intentionally very low to preserve the membrane integrity and architecture. This translates to a molar copolymer content below 6% of the total membrane composition of GPMV membrane, which is comparable to the content of cholesteryl-conjugated polymers reported for stabilization of liposome membranes by physical cross-linking (2.9%[62] and 4%[63]).

To evaluate whether the insertion of diblock copolymer and its cross-linking affected the GPMVs, we calculated the average size and size distribution of GPMVs, copolymer-supplemented GPMVs and cross-linked-copolymer GPMVs based on the CLSM images of more than 400 vesicles/GPMV type (Figure 3; Figure S10, Supporting Information). The average size of GPMVs was calculated as 6.1 ± 1.8 μm, while the values of the average size of copolymer-supplemented GPMVs were slightly smaller 5.8 ± 1.7, 5.6 ± 1.7, and 5.2 ± 1.6 μm, for applied copolymer concentrations of 0.1, 0.2, 0.25 mg mL^{-1}, respectively. The corresponding values for the cross-linked-copolymer GPMVs (5.7 ± 2.0, 5.6 ± 1.9, and 5.1 ± 1.5 μm) indicate that the copolymer cross-linking process did not affect the size of copolymer-supplemented GPMVs for the same copolymer concentrations. Based on the Student's *t*-test analysis, for an initial copolymer concentration of 0.1 mg mL^{-1}, no significant difference was observed between the size of copolymer-supplemented GPMVs/cross-linked-copolymer GPMVs and GPMVs ($P > 0.1$).

In order to investigate if our stabilization strategy can be extended to GPMVs from other cell lines, we produced and modified GPMVs derived from HeLa and MDA-MB-468 cells (Figure S10 and Videos S1–S3, Supporting Information). The successful membrane modification and the preserved integrity of these GPMVs is indicated by the bright fluorescent ring. In addition, their size is not significantly affected by copolymer insertion and cross-linking. The average sizes of GPMVs derived from HeLa and MDA-MB-468 were determined as 5.1 ± 1.6 and 4.9 ± 2.0 μm, respectively. After modification and cross-linking, the average GPMVs sizes were 4.9 ± 1.4 μm (HeLa) and 4.7 ± 1.7 μm (MDA-MB-468). These results demonstrate that our strategy could be applied for stabilization of GPMVs generated by different cell lines. However, HepG2 cells lacking of the membrane protein caveolae1 are particularly well suited for GPMV formation.[77] Therefore, we chose the GPMVs harvested from HepG2 cells as models to study the characteristics of cross-linked-copolymer GPMVs.

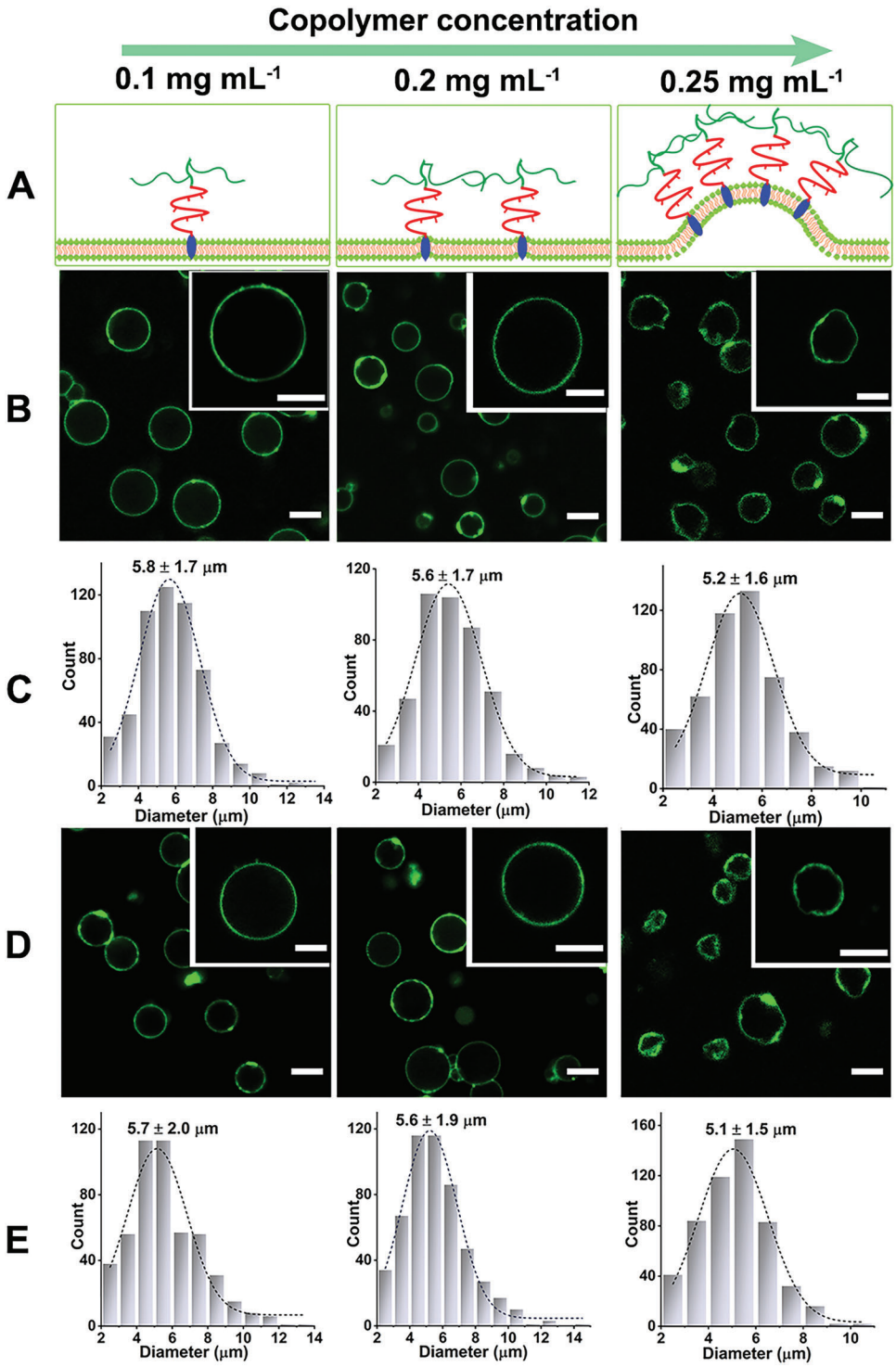

Figure 3. A) Schematic representation of possible membrane deformations with an increase of copolymer concentration (0.1, 0.2, and 0.25 mg mL^{-1}). CLSM images with the green fluorescent Atto-488 labeled copolymer B) copolymer-supplemented GPMVs and D) cross-linked-copolymer GPMVs (scale bar = 5 μm). Size distribution of C) copolymer-supplemented GPMVs and E) cross-linked-copolymer GPMVs obtained by analysis of CLSM images (400–500 GPMVs per sample). Statistical analysis: Student's *t*-test was performed to evaluate the effects of cross-linking on the size of GPMVs. Obtained two-sided *p*-values ($\alpha = 0.05$) were higher than 0.05, indicating nonsignificant differences between the studied samples ($P = 0.18$, 0.99, and 0.24 for 0.1, 0.2, and 0.25 mg mL^{-1} of copolymer concentration, respectively).

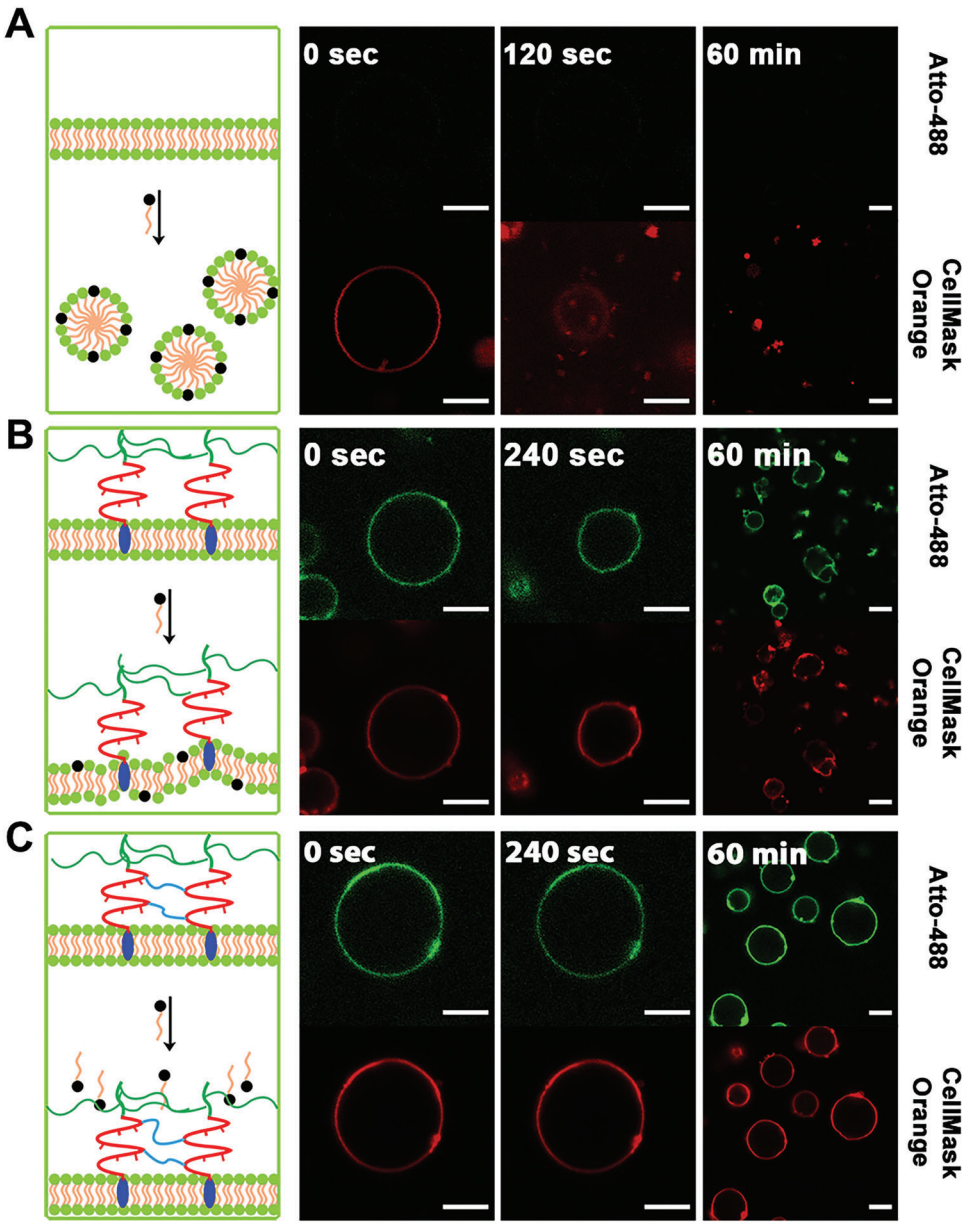

Figure 4. Influence of detergent (NP-40, 0.1%) on GPMV membrane morphology at various time points. Left column: schematic representation of GPMV membrane in the presence of NP-40. CLSM fluorescence images displayed in green (Atto-488 labeled copolymer) and red (CellMask Orange) of A) GPMVs, B) copolymer-supplemented GPMVs, and C) cross-linked-copolymer GPMVs. Scale bar = 5 µm. All experiments were performed in triplicate on different batches of GPMVs.

2.3. Resistance of the Cross-Linked-Copolymer GPMV Membranes to Surfactants

The efficiency of the cross-linking process on the membrane of GPMVs was investigated by addition of a surfactant, nonylphenyl-polyethylene glycol (NP-40), commonly used for cell membrane permeabilization.[78] To evaluate the stability of the GPMV membrane after the treatment with surfactant, we stained the membrane of native cells with CellMask Orange (5 µg mL^{-1}, 10 min) before the GPMV formation. By addition of NP-40, GPMVs changed within 120 s from a round vesicular architecture to a deformed structure (**Figure 4**A; Video S4, Supporting Information), which then started to disintegrate. After 60 min, only small dot-shaped objects were observed, indicating that NP-40 induced the complete GPMV membrane rupture over time. Membrane disruption occurred due to the insertion of surfactants into the phospholipid bilayer causing curvature stress and eventually lysis.[79] Similarly, membrane shrinking of copolymer-supplemented GPMVs occurred within 4 min from the addition of NP-40 (Figure 4B; Video S5, Supporting Information). After 60 min, only small, irregular vesicles remained. However, no significant difference in size and shape was observed for the

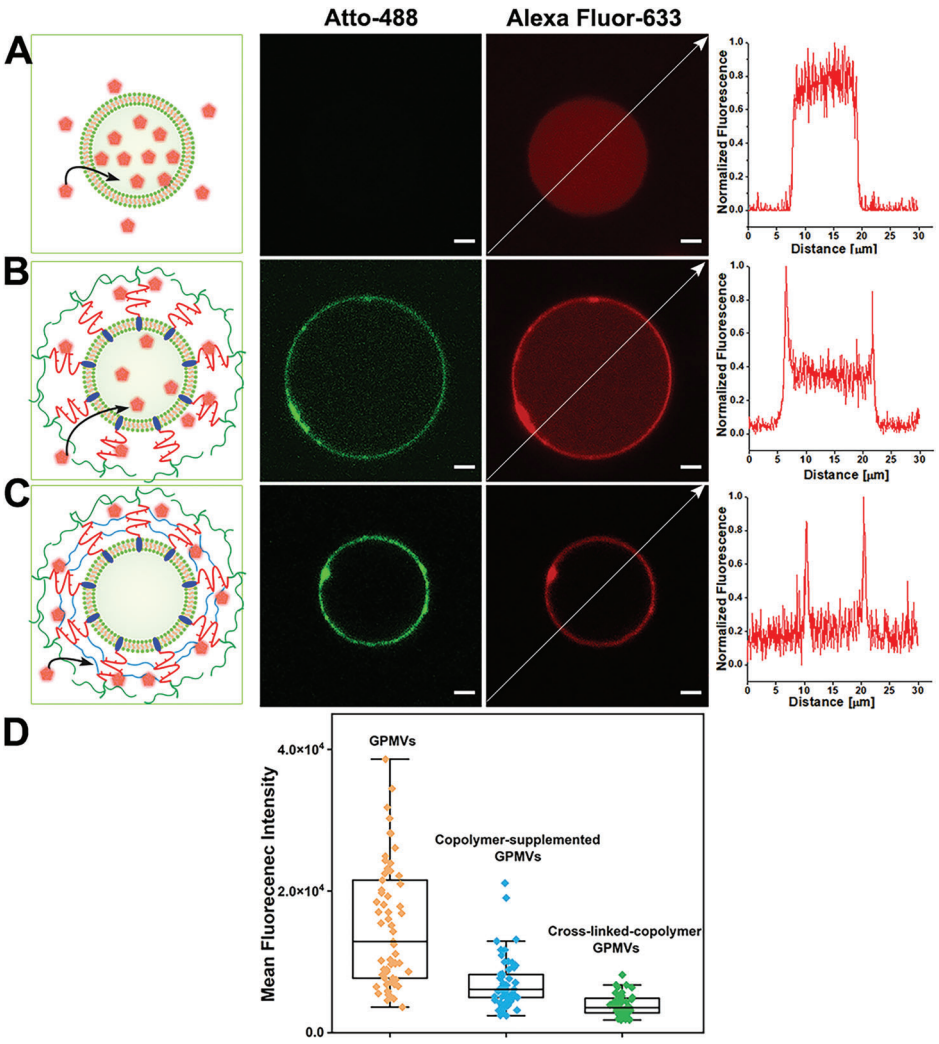

Figure 5. Effect of the membrane modification on the GPMV permeability. CLSM fluorescence images of A) GPMVs, B) copolymer-supplemented GPMVs, and C) cross-linked-copolymer GPMVs after incubation with Alexa Fluor-633-NHS-ester (0.05 mg mL^{-1}) at room temperature and pH 7.4. Left column: schematic representation. Middle: CLSM images of green and red fluorescence of Atto-488-labeled copolymer and Alexa Fluor-633, respectively. Right: plot profiles of red fluorescence across GPMVs diameter. Scale bar = 2 µm. Experiments were performed in triplicate on different batches of GPMVs. D) Mean fluorescence intensity of Alexa Fluor-633-NHS-ester dye permeated into the GPMVs, copolymer-supplemented GPMVs and cross-linked-copolymer GPMVs. One-way analysis of variance (ANOVA) test showed significant difference among all groups (p-values < 0.0001; n > 50). Mean fluorescence intensity and the plot profiles were obtained using the software ImageJ.

cross-linked-copolymer GPMVs after 60 min (Figure 4C; Video S6, Supporting Information). The preserved integrity of the cross-linked-copolymer GPMVs membrane after addition of the surfactant clearly shows that the membrane is sufficiently stabilized to resist rupture. This is not the case when the copolymer is inserted in the GPMV membrane without being cross-linked: the PEG side chains might entangle with each other but not in a stable manner which indicates copolymer cross-linking as the crucial step for membrane stabilization.

2.4. Effect of the Copolymer Cross-Linking on the GPMVs' Permeability

To study the effect of the copolymer cross-linking on the permeability of the GPMV membrane, we studied the permeation of molecules from the environment for all three kinds of GPMVs. Specifically, a hydrophilic dye, Alexa Fluor-633-NHS-ester, was added at pH 7.4 to GPMVs, copolymer-supplemented GPMVs and cross-linked-copolymer GPMV dispersions. CLSM images and fluorescence profile of GPMVs show that Alexa Fluor-633-NHS-ester permeates through the membrane and exhibits homogeneous high red fluorescence intensity inside of the GPMVs due to the NHS coupling to internal proteins (**Figure 5**A; Figure S11A, Supporting Information).[80] In the case of copolymer-supplemented GPMVs, Alexa Fluor-633-NHS-ester permeates inside GPMVs and, in addition, is interacting with the copolymer, as observed by the highly intense fluorescent ring associated with the GPMV membrane (Figure 5B; Figure S11B, Supporting Information). Dye accumulation on the GPMV membrane can be explained by reaction of Alexa Fluor-633-NHS-ester with the free amine groups of the copolymer. On the contrary, after

cross-linking, Alexa Fluor-633-NHS-ester did not permeate through the membrane of the cross-linked-copolymer GPMVs and remained only in the GPMV membrane due to the possible interaction with the remaining free amino groups of the copolymer (Figure 5C; Figure S11C, Supporting Information). The cross-linked polymer shell at the external interface of GPMVs prohibits the dye permeation and therefore serves to retain the original GPMV cargo composition as an important step for further development of applications. The results represent the statistical analysis of the mean fluorescence intensity for more than 50 vesicles from each type of GPMVs (Figure 5D). Besides this, the interaction of cross-linked-copolymer GPMVs with Alexa Fluor-633-NHS-ester indicates that the cross-linking procedure does not involve all free amino groups exposed on the copolymer, which allows their usage for further conjugation in more advanced systems.

Then, we investigated the leakage of molecules from GPMVs and cross-linked-copolymer GPMVs using Atto-633, a water-soluble fluorescent dye as a "reporting" molecule. First, GPMVs were mixed with an Atto-633 solution (0.025 mg mL^{-1}) for 10 min followed by washing out the excess dye. Next, we inserted the Atto-488-labeled Chol-PAEMA-PEGMA copolymer into Atto-633-loaded GPMVs, and cross-linked the copolymer. The fluorescence intensity of Atto-633 inside the cross-linked-copolymer GPMVs was measured over time and compared with that inside the GPMVs. Whilst the relative fluorescence intensity of Atto-633 inside GPMVs decreased by 63%, in cross-linked-copolymer GPMVs, this decreased only by 18% under the same conditions (Figure S12A–C, Supporting Information). In order to evaluate the reduction of the fluorescence intensity caused by photobleaching of the dye, we measured the fluorescence intensity of Atto-633 in GPMVs under similar laser power conditions and took it into account for a background correction (Figure S12D, Supporting Information). As the relative fluorescence intensity of Atto-633 was reduced by 12% in the same exposure time, it indicates that a significant fluorescence reduction is caused by photobleaching. Therefore, the decrease in fluorescence intensity of the dye when encapsulated inside cross-linked-copolymer GPMVs is mainly due to photobleaching of the dye, and not to a dye release. Although, encapsulated molecules can diffuse across the GPMV membrane through membrane protein channels,[81] the cross-linking step can effectively reduce molecule leakage from GPMVs. Insertion and cross-linking of the diblock copolymer not only enhanced the stability of GPMVs but also significantly reduced the permeation of molecules from the environment into their cavity or the escape of encapsulated molecules. Taken together, our approach provides a promising platform for preparing cell-derived vesicles with reduced membrane permeation at neutral pH that can be further developed for cell mimics or drug delivery applications.

2.5. Stability of GPMVs at 4 °C and Physiological Temperature

Stability is one of the most important factors for controllable in vitro and in vivo therapeutic applications of cell-derived vesicles.[82] To get more details regarding the stability of cross-linked-copolymer GPMVs, we investigated their ability to maintain the membrane integrity under different storage and environment conditions. Specifically, we analyzed the stability of GPMVs, copolymer-supplemented GPMVs and cross-linked-copolymer GPMVs at 4 °C (**Figure 6**). Initially, all types of GPMVs preserved their morphology without any aggregation. Then, GPMVs slowly aggregated after 14 days, while cross-linked-copolymer GPMVs still preserved their integrity without aggregation for at least 28 days. As expected, the presence of the PEGMA block at the exterior of the GPMVs effectively prevents the aggregation of GPMVs. Extracellular vesicles were also reported to suffer from aggregation and flocculation in physiological saline solutions, which limits their long-term storage.[83] The polymer modification of the cell membrane in vesicles generated by donor cells represents an elegant and straightforward manner to increase the stability and quality of stored membranes while preserving their morphology.

The membrane of GPMVs was reported as less rigid at physiological temperature (37 °C) than at RT,[84] as higher temperatures induce fluidization of membranes and eventually disintegrates the lipid bilayers.[85] In order to investigate the membrane morphology of GPMVs, copolymer-supplemented GPMVs and cross-linked-copolymer GPMVs at physiological temperature (37 °C), we stored all GPMVs (stained with CellMask Green) at 37 °C for one week. The CLSM images revealed that the GPMV membrane and the copolymer-supplemented GPMVs membrane ruptured: the former into small fragments (**Figure 7**A), while the copolymer-supplemented GPMVs formed aggregates (Figure 7B). Interestingly, the cross-linked-copolymer GPMVs preserved their membrane integrity after one week of storage at physiological temperature (Figure 7C). This demonstrates that the cross-linked polymer shell effectively improves the stability of the GPMV membrane for periods of time longer than required for in vivo applications and thus overcomes the limitation of inherently fragile GPMVs use in in vivo studies.

2.6. Mechanical Properties of Cross-Linked-Copolymer GPMVs

Investigation of the mechanical properties of GPMVs is essential to gain a deeper understanding of the fundamental biological mechanisms, which could facilitate their technological applications such as diagnostics and therapeutics. To calculate the mechanical properties, we used vesicle fluctuation analysis. This method is generally applied to extract information about physical properties of membranes.[86] To measure the thermal shape fluctuations of giant lipid vesicles, we captured images with a high frame rate by CLSM and processed them, yielding the mean amplitude of the Fourier fluctuation modes spectrum. By comparison with a theoretical model of an expected Boltzmann distribution, it allows to determine the bending rigidity (κ_b) of the membrane. The bending rigidity is highly sensitive to membrane changes as the bending elastic modulus depends strongly on the membrane thermodynamic state and composition.[84] To investigate if the copolymer cross-linking process affected the bending rigidity of GPMVs, we stained the GPMV membranes with a hydrophobic fluorescent dye (BODIPY 630/650-X Succinimidyl Ester). Then, we recorded the fluctuations of the membrane by using CLSM (Videos S7–S9, Supporting Information). The CLSM images of membrane fluctuations obtained for GPMVs display

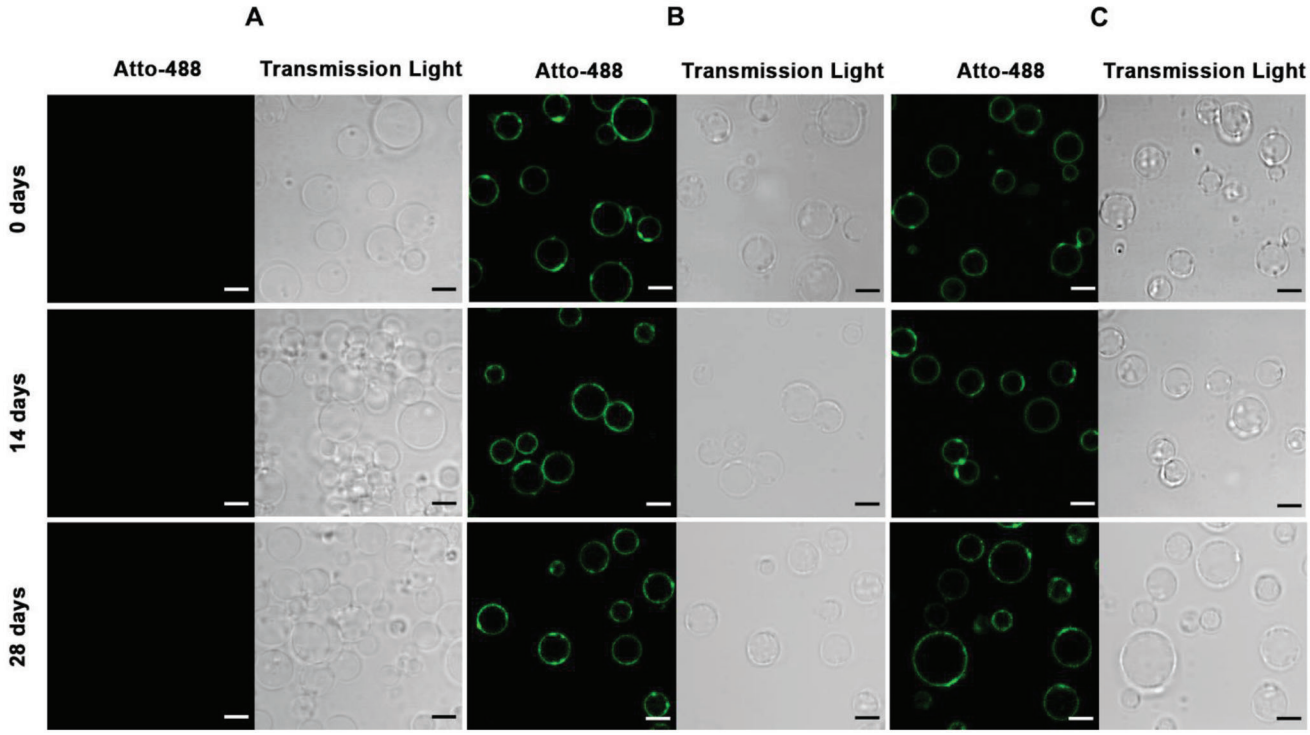

Figure 6. Stability of GPMVs upon storage at 4 °C. CLSM images display green fluorescence of Atto-488 labeled Chol-PAEMA-*b*-PEGMA (Atto-488) and transmission light. A) GPMVs, B) copolymer-supplemented GPMVs, and C) cross-linked-copolymer GPMVs stored for 0, 14, and 28 days. Scale bar = 5 µm.

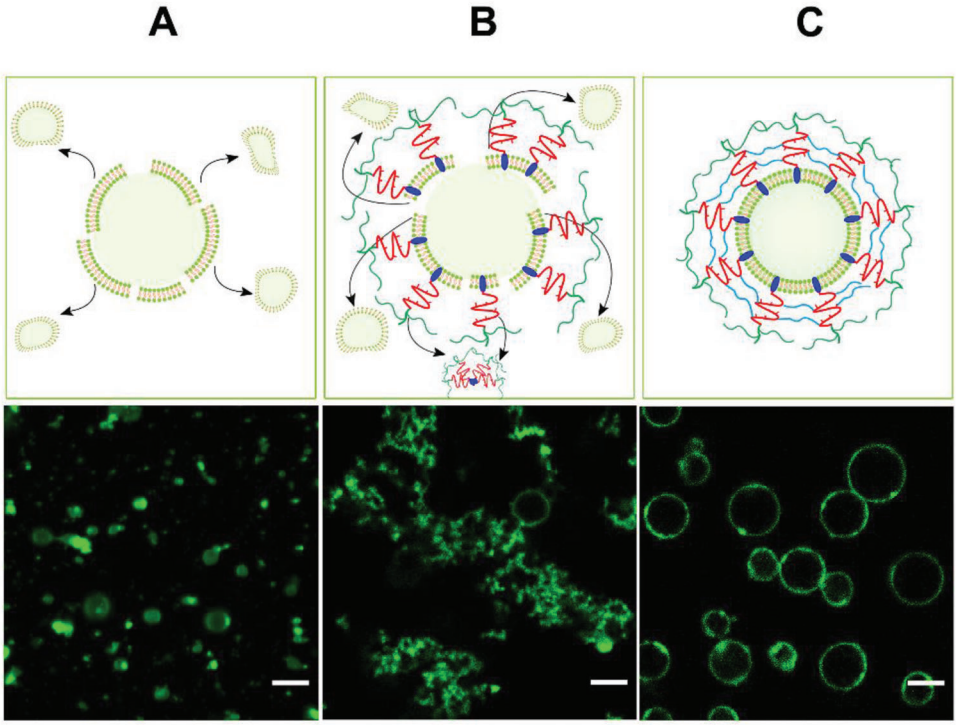

Figure 7. Stability of GPMVs at 37 °C. A) GPMVs, B) copolymer-supplemented GPMVs, and C) cross-linked-copolymer GPMVs. Top: schematic representation of the influence of storage at elevated temperature on the membrane of GPMVs. Bottom: CLSM fluorescence images of GPMVs after 7 days of storage at 37 °C. A) Cell Mask Green, B,C) Atto-488 labeled copolymer. Scale bar = 5 µm.

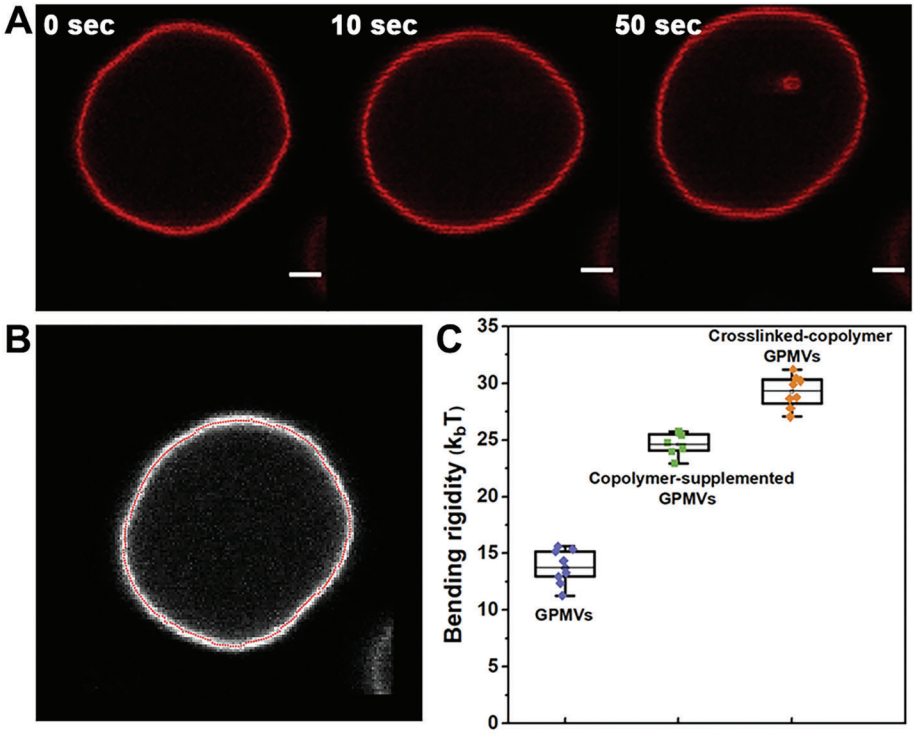

Figure 8. Bending rigidity measurements of cross-linked-copolymer GPMVs by analysis of thermally induced membrane fluctuation. A) Time lapse CLSM images of a cross-linked-copolymer GPMV fluctuation. Red: BODIPY 630/650-X Succinimidyl Ester. Scale bar = 2 µm. B) The detected membrane contour (red) is shown as overlay on the CLSM image. The bending rigidity κ_b of this cross-linked-copolymer GPMV is 30.5 ± 3.0 k_BT. C) Bending rigidity values for unmodified and modified GPMVs. One-way analysis of variance (ANOVA) test showed significant difference among all groups (p-values < 0.0001).

significant fluctuation of the vesicles (**Figure 8**A). We analyzed membrane fluctuations around the mean spherical shape (Figure 8B), then extracted both the decay time and a decay constant, L_m, of each Fourier fluctuation mode (Figure S13, Supporting Information). The bending rigidity values were obtained by analyzing 8–9 vesicles for each sample (Figure 8C). Polymer incorporation stiffened the membrane, the bending rigidity of copolymer-supplemented GPMVs increased almost twofold compared to that of GPMVs, from $\kappa_b = 13.8 \pm 2.4\ k_BT$ to $\kappa_b = 24.6 \pm 1.9\ k_BT$. Cross-linking the copolymer resulted in even more robust membranes with a bending rigidity value of 29.3 ± 2.3 k_BT. The material property of bending rigidity describes the energetic cost of membrane deformations and its resistance to bending.[84] After the modification and cross-linking of copolymer, the GPMV membranes show a higher bending rigidity, indicating a high energetic cost for membrane deformation and a larger resistance to bending. Given the experimental errors, polymer insertion and cross-linking effectively improved the stability of GPMVs. The bending rigidity is corelated to membrane fluidity which describes the diffusion of lipids and proteins in the membrane.[87] A more rigid membrane is associated with a lower membrane fluidity.[84,88] In biology, the membrane fluidity refers to the viscosity of the lipid bilayer of a cell membrane.[89] Thus, we expect that cross-linking of the copolymer on the GPMV membrane not only increases the bending rigidity but also reduces the membrane fluidity.

Interestingly, the bending rigidity value significantly increased after the insertion of Chol-PAEMA-*b*-PEGMA diblock copolymers into the GPMV membrane, whereas the covalent cross-linking of the copolymer had a lower effect. The insertion of cholesteryl anchors has been reported to contribute to the increase of lipid membrane stiffness.[84] In addition, as the density of tethered polymer chains is affected by interpolymer chains interactions, interactions with the surface, and with the solvent,[90] it is necessary to analyze the possible conformation of the anchored copolymer chains. To model the possible conformations of the PAEMA-*b*-PEGMA chains, we estimated the length of the copolymer brushes exposed at the surface of GPMVs using Flory approximation.[91] This model evaluates changes in conformation of an ideal random-walk polymer by the presence of solvent molecules, the constraint induced by tethering one end of the polymer chain on a surface and the increase in grafting density.[91–93] PEG side chains of the hydrophilic PEGMA block are expected to adopt a stretched brush conformation in aqueous solution (Figure S14, Supporting Information) due to formation of hydrogen bonds, which favor local overlapping and entanglement. This interaction between the relatively long PEG side chains will induce a physical cross-linking of the polymer layer that induces a significant increase in the bending rigidity of the copolymer-supplemented GPMVs. On the other hand, the PAEMA block tends to adopt an elongated coil conformation due to the spatial restrictions determined by both the anchoring of the cholesteryl terminal groups into the GPMV membrane and the connection of the other chain end to the PEGMA block (details in the Supporting Information). Therefore, the access of PFA to the amine groups of PAEMA is affected by the decreased

accessibility of the moieties available for interaction and the distance between the adjacent copolymer chains. While contributing to bending rigidity of the copolymer-supplemented GPMV membrane, the physical cross-linking of the PEGMA block affects the covalent cross-linking density, which might explain the moderate increase in membrane bending rigidity. However, the covalent cross-linking process plays an essential role in the stability and permeability of the GPMVs membrane. The covalent bonds formed by chemical cross-linking are sufficient to make the GPMV membrane impermeable for small molecules (e.g., dyes) and significantly more resistant against surfactants.

Synthetic lipid membranes are considered to be more robust than GPMV membranes as the high membrane protein content in GPMVs has been reported to reduce the bending rigidity.[94–96] In fact, their bending rigidity values not only depend on the measuring technique but also on the environmental conditions (i.e., immersing medium and the presence of various molecules and salts).[97] To minimize the effect of the environment on bending rigidity, we selected the 1-palmitoyl-2-oleoyl-sn-glycero-3-phosophocholine (POPC) lipid membranes, which were measured under conditions similar to those of GPMV membranes. We compared the bending rigidity of POPC lipid membranes[98,99] with that of GPMV membranes and as expected, the bending rigidity of GPMV membranes was lower than that of pure POPC GUVs (Table S2). Our cross-linked-copolymer GPMV membranes were more robust than the native GPMV membranes, resulting in a bending rigidity of $29.3 \pm 2.3\ k_B T$, similar to that of pure POPC membranes.

2.7. Effect of the Cross-Linked-Copolymer GPMVs on Cell Viability

To assess the bioapplicability of obtained vesicles, we investigated the influence of GPMVs, copolymer-supplemented GPMVs, cross-linked-copolymer GPMVs and various concentrations of block copolymer on the viability of HeLa cells (Figure S15, Supporting Information). As expected, GPMVs, as cell-derived vesicles, were not cytotoxic. Interestingly, neither the copolymer-supplemented GPMVs nor the cross-linked-copolymer GPMVs displayed cell toxicity after the removal of PFA.

Together with their intrinsic complex composition comprising of a variety of lipids and proteins as inherited from the donor cells, the cross-linked-copolymer GPMVs represent an ideal candidate for both fundamental studies and advanced applications. Although the equipment of GPMVs with cholesteryl-functionalized PEG chains has been previously reported by our group,[49] here we go one step further: we achieved an improved mechanical stability of the membrane by cross-linking the specifically designed copolymer. In addition, we preserve both the GPMVs integrity and the lack of toxicity as key aspects for the in vitro and in vivo application of GPMVs.

2.8. pH-Triggered Membrane Permeabilization of Cross-Linked-Copolymer GPMVs

To evaluate the "on-demand" GPMV functionality after the cross-linking of the copolymer, we investigated the molecular transport across the GPMV membrane at slightly acidic pH values (6.0–6.5). First, we studied the permeation of molecules from the environment both for GPMVs and cross-linked-copolymer GPMVs. Specifically, a hydrophilic dye, Alexa Fluor-633-NHS-ester, was added to GPMVs and cross-linked-copolymer GPMV dispersions at pH 7.4. The CLSM images and the fluorescence profile of cross-linked-copolymer GPMVs indicate no dye permeation through the membrane (Figure 5A). However, when the pH value decreased to 6.0, the mean fluorescence intensity of Alexa Fluor-633-NHS-ester inside of GPMVs and cross-linked-copolymer GPMVs increased significantly, and a homogeneous red fluorescence intensity was observed (Figure S16, Supporting Information) indicating that the dye molecules could easily permeate the membrane. At acidic pH, the cross-linked polymer layer swells due to the electrostatic repulsion between the protonated primary amine moieties, which favors the access of the dye molecules to the transmembrane proteins of GPMVs. By contrast, the membrane of native GPMVs ruptured after 3 h of incubation at pH 6.0 (Figure S17, Supporting Information).

We further investigated the release of a hydrophilic dye, Atto-633, from the cross-linked-copolymer GPMVs. The dye was prior loaded into the native GPMVs at pH 7.4 (before copolymer insertion and cross-linking). The CLSM images clearly showed that the cross-linking step is of a key importance in preventing the leakage of encapsulated molecules from GPMVs (Figure S12, Supporting Information). In response to the decrease of pH down to 6.5, the dye was released very fast in the first 10 s (Video S10, Supporting Information), and after 1 h, no fluorescence was observed anymore inside of GPMVs (Figure S18, Supporting Information). The results provide significant evidence for the pH-induced permeation/release of molecules into and from the cross-linked-copolymer GPMVs while preserving their architectural integrity.

2.9. The Functionality of Cross-Linked-Copolymer GPMVs

We considered essential for further applications to investigate the accessibility of surface membrane molecules of GPMVs (i.e., receptors, cell markers) to the interaction with ligands or antibodies, after modification of GPMVs with the copolymer and cross-linking. We followed the immunofluorescent detection of epidermal growth factor receptor (EGFR) on the membrane of native GPMVs and cross-linked-copolymer GPMVs, respectively. We used GPMVs derived from MDA-MB-468 cells (with a high EGFR expression)[100] and compared with GPMVs generated by HepG2 cells (with a low EGFR expression)[101] as a negative control. The difference of EGFR expression between these two cell lines was first indicated by the antibody staining performed on the fixed cell samples (Figure S19, Supporting Information). Then, we used the antibody staining on the corresponding GPMVs and cross-linked-copolymer GPMVs to show the accessibility of receptors after the membrane modification and cross-linking (**Figure 9**; Figure S20, Supporting Information).

The intensity of the fluorescence signal from the GPMVs and cross-linked-copolymer GPMVs, derived from highly EGFR expressing cell line serves to observe the antibody binding. The stabilization of GPMV membrane with the cross-linkable block copolymer does not block the interaction with the antigens or receptors present on the surface of cell membrane. Therefore,

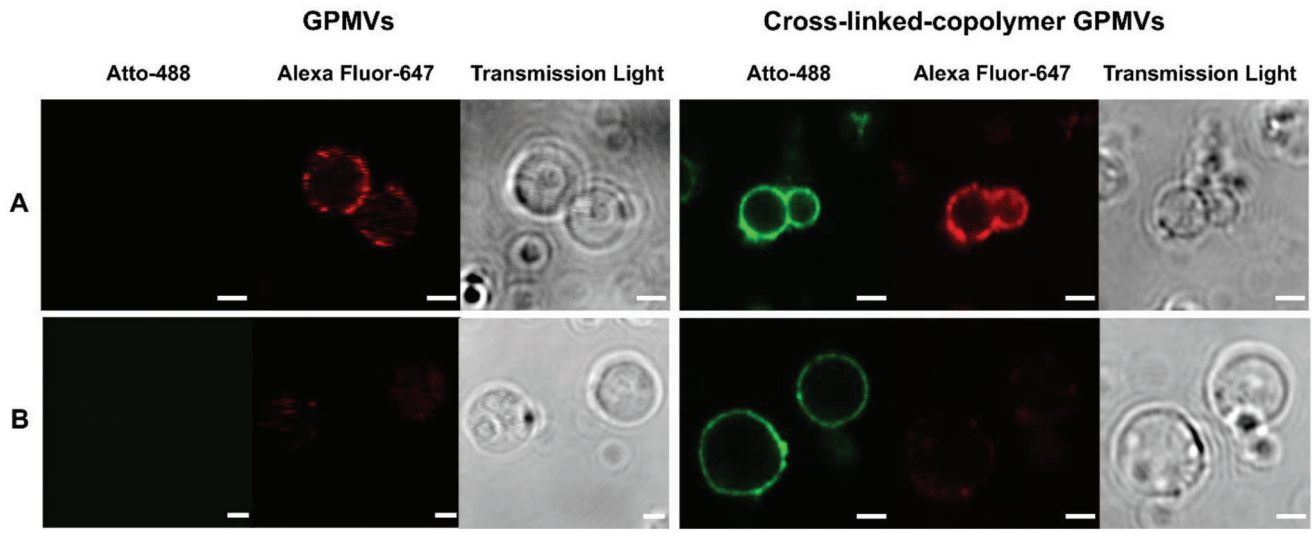

Figure 9. Immunofluorescent staining of EGFR on GPMVs membrane. CLSM images of fluorescently stained native GPMVs (left panel) and cross-linked-copolymer GPMVs (right panel) derived from A) MDA-MB-468 cells and B) HepG2 cells. Channels represent the green fluorescence of Atto-488 stained copolymer (Atto-488), the red fluorescence of immunofluorescently stained EGFR (Alexa Fluor-647), and the transmitted light. Scale bars = 2 µm.

our strategy supports further bioapplications involving specific receptor–ligand or antigen–antibody interactions.

3. Conclusions

The evolution of biomedical applications, including drug delivery or molecular factories, relies on the development of cell-derived vesicles as they provide ideal bioinspired platforms to construct cell mimics, develop advanced therapeutic carriers or study the lipid/protein behavior of cell membranes. Here, we introduce an elegant strategy to overcome the major limitations associated with the inherent fragility and aggregation of cell-derived vesicles, including GPMVs, by the insertion of a specifically designed copolymer into the membrane and the subsequent cross-linking of the copolymer. In addition, the specific selection of the copolymer inserted in the GPMVs membrane and cross-linked served to induce an emerging property: stimuli-responsiveness of the membrane. RAFT polymerization allowed for the synthesis of a well-defined Chol-PAEMA-*b*-PEGMA diblock copolymer, which was successfully inserted into the membrane of GPMVs due to the cholesteryl terminal groups acting as anchoring moieties. The unique advantages of equipping GPMVs with a cross-linkable, pH-responsive copolymer are the significant improvement in membrane stability, avoiding their aggregation over time, and stimuli-responsive permeability of the GPMV membrane. Indeed, by combining surfactant-induced membrane disruption and dye permeation assays, we observed that the cross-linked-copolymer GPMVs were more stable at neutral pH than the native GPMVs and significantly hindered molecular transport through the membrane. Both qualities are key aspects for further development of bioapplications. Interestingly, the insertion of Chol-PAEMA-*b*-PEGMA diblock copolymer into the membrane has a higher effect on the bending rigidity than the covalent cross-linking of the PAEMA blocks. We explained this difference by the increased hydrophilicity of PEGMA blocks that introduce hydrogen bonds between the PEG side chains favoring local overlapping and entanglement of the chains. The higher interaction between the PEG side chains leads to a physically cross-linked polymer layer inducing an increase in the bending rigidity of the copolymer-supplemented GPMVs membrane. On the other hand, the covalent cross-linking is additionally increasing the GPMV membrane integrity and represents the real factor preventing both the membrane leakage and rupture in the presence of surfactants. Importantly, both copolymer-supplemented GPMVs and cross-linked-copolymer GPMVs showed no cytotoxicity. Together with their cytoplasm and membrane composition inherited from the donor cells, cross-linked-copolymer GPMVs are ideal candidates to support advanced application by complex reactions in a nature-like manner. To the best of our knowledge, this is the first example of copolymer-stabilized cell-derived giant vesicles capable to trigger the permeation of molecules across their membrane in a pH-mediated manner. In addition, as the membrane stability and architectural integrity were preserved for more than two weeks of storage under different conditions, including room temperature, our strategy produces robust biomimetic membranes endowed with a stimuli-triggered functionality. Taken together, the cross-linked-copolymer GPMVs have a high potential in developing new solutions for advanced therapies.

4. Experimental Section

Materials: CPDB (95%), DCC (99%), DMAP (≥99%), (2-boc-amino) ethyl methacrylate (99%), 2,2′-azobis(2-methylpropionitrile) (AIBN) (98%), PEGMA (M_n = 480), Atto-488-NHS-ester (≥80%), PFA powder (95%), and the organic solvents used in the project were purchased from Sigma-Aldrich. The AIBN was recrystallized twice from methanol before use. Dialysis membranes were obtained from Spectrum Laboratories, Inc. CellMask Green Plasma Membrane Stain, Alexa Fluor 633 Carboxylic Acid Succinimidyl Ester, Atto-633 and BODIPY 630/650-X Succinimidyl Ester, WGA-Alexa Fluor 555 conjugate and Alexa Fluor 647 donkey antimouse IgG polyclonal antibody were purchased from ThermoFisher, anti-EGFR

monoclonal antibody was purchased from BD Biosciences. GPMV buffer (10 mM HEPES, 150 mM NaCl, 2 mM $CaCl_2$, pH 7.4) was filtered and stored at 4 °C.

Synthesis of Cholesteryl-Terminated RAFT Agent: Cholesterol (500 mg, 1.3 mmol), CPDB (433.5 mg, 1.6 mmol), DCC (400 mg, 1.9 mmol), and DMAP (2 mg, 0.02 mmol) were mixed and stirred overnight in dry $CHCl_3$ at room temperature, under argon atmosphere. The solid precipitate was separated by filtration and the solvent was removed by evaporation. The residue was purified by silica gel column chromatography using hexane/ethyl acetate (12/1) as eluent to afford a pink oil (0.393 g) with a yield of 46.7%.

Synthesis of Chol-PBocAEMA: Chol-PBocAEMA was synthesized via RAFT polymerization. Briefly, (2-Boc-amino) ethyl methacrylate (1.0 g, 4.36 mmol), cholesteryl-terminated RAFT agent (96.8 mg, 0.14 mmol), and AIBN (4.8 mg, 0.03 mmol) were dissolved in DMF (5 mL). The solution was deoxygenated for 30 min by bubbling with argon and then immersed in a 70 °C bath for 12 h under argon atmosphere. The resulting copolymer was dropped into ethyl ether to precipitate and then filtered. The filtrate was concentrated and dissolved in DCM, then the solution was dried to afford a pink solid (0.797 g) with a yield of 73%. ^{1}H NMR spectroscopy indicated a mean degree of polymerization of 20 for the Chol-PBocAEMA (calculated by comparing the integrated signals corresponding to the aromatic protons at 7.2–8.0 ppm with those assigned to the Boc-protective group at $\delta = 1.4$ ppm).

Synthesis of Chol-PBocAEMA-b-PEGMA: Chol-PBocAEMA (150 mg, 0.028 mmol), PEGMA (190 mg, 0.39 mmol), and AIBN (2 mg, 0.012 mmol) were dissolved in DMF (5 mL). The solution was deoxygenated via bubbling with argon for 30 min, and then placed in an oil bath at 70 °C for 12 h. The resulting diblock copolymer was collected and filtered by precipitation from ethyl ether. The filtrate was transferred to DCM and dried to get a pink product (0.301 g) with a yield of 84%. The block ratio was determined by integrating the BocPAEMA side chain (Boc) at $\delta = 1.4$ ppm as a reference and the peaks of the PEGMA side chain at $\delta = 3.6$ ppm attributed to the O–CH_2–CH_2 protons.

N-Boc Deprotection: TFA (5 mL) was added to a solution of Chol-PBocAEMA-*b*-PEGMA (221 mg, 0.02 mmol) in DCM and the mixture was stirred for 4 h at RT. After evaporation of the solvent, the mixture was dissolved in MilliQ water and dialyzed against NaOH solution (0.1 M) using a dialysis membrane with a molecular weight cut-off of 3.5 kDa (the solution was exchanged four times). Finally, Chol-PAEMA-*b*-PEGMA (0.103 g) was obtained after freeze-drying with a yield of 58%.

Atto-488 Labeled Chol-PAEMA-b-PEGMA: To label the copolymer, Chol-PAEMA-*b*-PEGMA (100 mg), Atto-488-NHS-ester (50 µL, 1 mg mL^{-1}), and triethylamine (10 µL) were dissolved in DMSO and stirred overnight at RT. The mixture was purified by dialysis in MilliQ water using a 3.5 kDa molecular weight cut-off membrane (the solution was exchanged four times), and the dye-labeled polymer was obtained after freeze-drying. Atto-488 labeled Chol-PAEMA-*b*-PEGMA (10 mg) was dissolved in GPMV buffer to prepare a stock solution.

1H Nuclear Magnetic Resonance Spectroscopy: ^{1}H NMR spectra were recorded in deuterated solvents $CDCl_3$, CD_2Cl_2-d or D_2O (purchased from Cambridge Isotope Laboratories USA) on a Bruker Avance III NMR spectrometer operating at a frequency of 500 MHz. Chemical shifts (δ) are reported in ppm, whereas the chemical shifts were calibrated to the main solvent residual peaks. The collected spectra were analyzed using MestReNova (v9.1) (Mestrelab Research S.L.).

GPC: GPC calibrated with narrow-distributed polystyrene standards was applied to determine the average molecular weight and dispersity ($Đ$) of the diblock copolymer. GPC measurements using chloroform as eluent were recorded on an Agilent infinity 1200 system (Polymer Standard Services, Germany) equipped with a refractive index detector and a series of linear-S SDV columns. The temperature of all columns was set to 35 °C and a flow rate of 1.0 mL min^{-1} was used.

Confocal Laser Scanning Microscopy: CLSM measurements were performed using an LSM 880, inverted microscope ZEISS Axio Observer (Carl Zeiss, Germany) with a water immersion objective (C-Apochromate 40×/1.2 W korr FCS M27). Samples containing Atto-488 were excited with a 488 nm argon laser collecting the fluorescence in the range of 499–629 nm. Atto-633, Alexa Fluor-633-NHS-ester, and BODIPY 630/650-X Succinimidyl Ester were excited with a 633 nm HeNe-laser collecting fluorescence in a range of 638–759 nm. Each sample was scanned unidirectionally using 512 × 512 pixels with a Bit depth of 8 Bit. Images were processed using ImageJ (1.53c).

Cell Culture and GPMV Formation: HepG2 and HeLa cells were cultured in Dulbecco's Modified Eagle's Medium and MDA-MB-469 cells were cultured in RPMI-1640. Culture media were supplemented with 10% fetal bovine serum and 1% penicillin–streptomycin. Cell cultures were maintained in an incubator at 37 °C with 5% CO_2. GPMVs were produced and isolated from the cells, as previously described.[39,49,77] To produce GPMVs, cells were seeded in a 6-well cell culture plate with a density of 1.5×10^5 cells per well. After growing the cells to a confluency of 70% to 90%, cells were washed three times with GPMV buffer. Membrane vesiculation was then induced by incubation of cells with vesiculation buffer consisting of PFA (25 mM) and DTT (2 mM) in GPMV buffer for 2 h at 37 °C. Then, the supernatant (500 µL) from each well was transferred to an Eppendorf tube and centrifuged at 0.1 rpm for 10 min to remove cells, then twice at 16 100 × *g* for 1 h at 4 °C to collect and wash GPMVs with GPMV buffer. GPMVs were dipersed in a concentration of 1.6×10^6 mL^{-1} and transferred to a plasma activated 8-well chambers slide (Nunc Lab-Tek Chamber Slide System, Thermo Fisher Scientific). The concentration of GPMVs was estimated by CLSM. Specifically, GPMVs solution (200 µL) was added to an 8-well chamber (area per well: 0.7 cm^2) and left two days for sendimentation. Five images with a size of 212.5 µm × 212.5 µm were taken using CLSM and the average number of GPMVs per image area was determined. Total number of GPMVs mL^{-1} = (average number of GPMVs per image/image area) × area of a well (0.7 cm^2) × 5.

Modification of GPMV Membranes by Insertion of Atto-488 Labeled Chol-PAEMA-b-PEGMA and Cross-Linking the Diblock Copolymer: Copolymer-supplemented GPMVs were prepared by addition of Atto-488 labeled Chol-PAEMA-*b*-PEGMA (final concentration: 0.1, 0.2, and 0.25 mg mL^{-1}) to the GPMVs solution (200 µL) in an 8-well chambers slide (around 3.2×10^5 GPMVs per well). After 20 min, the copolymer-supplemented GPMVs were washed five times with GPMV buffer to remove unbound copolymer. Copolymer-supplemented GPMVs were cross-linked by addition of PFA (0.4%). After 30 min, the resulting GPMVs were washed five times with GPMV buffer to remove the free PFA. Copolymer-supplemented GPMVs and cross-linked-copolymer GPMVs were prepared using a copolymer concentration of 0.2 mg mL^{-1} in the next experiments, while in the dye permeation study, the GPMVs were modified with a copolymer concentration of 0.1 mg mL^{-1}.

Surfactant Resistance Study: Surfactant resistance was performed by addition of nonylphenyl-polyethylene glycol (NP-40). Before GPMV formation, cell membrane was stained with CellMask Orange (5 µg mL^{-1}, Invitrogen, USA) for 10 min. Then, GPMVs, copolymer-supplemented GPMVs and cross-linked-copolymer GPMVs were formed using the method mentioned above. Subsequently, the NP-40 solution was added to the three kinds of GPMVs to reach a final concentration of 0.1%. CLSM images were taken immediately after the addition of NP-40.

Dye Permeation Study: Dye permeation was investigated by addition of Alexa Fluor-633-NHS-ester (final concentration: 0.05 mg mL^{-1}) to GPMVs, copolymer-supplemented GPMVs, and cross-linked-copolymer GPMVs. All GPMVs were washed five times with GPMV buffer after a treatment of 30 min and CLSM images were taken afterward. All permeation experiments were performed at room temperature. Images were processed with ImageJ2. GPMVs were only considered if their diameter was more than 5.2 µm. An overlay diameter of 4.8 µm was applied to each GPMV to measure the mean fluorescence intensity inside.

Dye Leakage Assay: GPMVs were incubated for 10 min with water-soluble fluorescent dye-Atto-633 (final concentration: 0.025 mg mL^{-1}) and subsequently washed five times with GPMV buffer to remove the free dye. The cross-linked-copolymer GPMVs were prepared in three steps. First, GPMVs were incubated with Atto-633 solution (final concentration: 0.025 mg mL^{-1}) for 10 min and washed once with GPMV buffer to remove excess of the dye. Second, Atto-488 labeled Chol-PAEMA-*b*-PEGMA copolymer was added to reach a final concentration of 0.2 mg mL^{-1}. After 20 min of incubation, the unbound polymer was removed by washing

twice with GPMV buffer. Third, PFA (final concentration: 0.4%) was used for polymer cross-linking and incubated for 30 min with subsequent washing of free PFA by GPMV buffer. CLSM images of all samples were taken every 5 min for 100 min. Fluorescence intensity was measured for individual GPMVs using ZEN black (v2.3). To determine the photobleaching effect of the fluorescent dye, Atto-633-loaded GPMVs were imaged using the same laser power but continuously without break intervals between the time points (100 s in total). The leakage assay was performed at room temperature.

Stability of GPMVs under Storage at 4 °C and Physiological Temperature (37 °C): GPMVs, copolymer-supplemented GPMVs, and cross-linked-copolymer GPMVs were stored at 4 and 37 °C in GPMV buffer to investigate their stability: CLSM images were taken before storage, after 14 and 28 days of storage (4 °C) or after 7 days (37 °C).

Membrane Bending Rigidity: Membrane bending rigidity was measured by fluctuation analysis of the thermally induced motion of the GPMV membrane. Statistical analysis was performed in MATLAB using an approach described by Spanke et al.[86] GPMVs, copolymer-supplemented GPMVs, and cross-linked-copolymer GPMVs were prepared with unlabeled Chol-PAEMA-*b*-PEGMA and then incubated with BODIPY 630/650-X Succinimidyl Ester (final concentration: 12.5 µM). After washing five times with GPMV buffer, sucrose (final concentration: 75 mM) was added to GPMVs solution for optically resolvable membrane fluctuation, and then a video of 5000 images was recorded at 51 frames per second (fps). Subsequently, bending rigidity values were analyzed with an ANOVA test to assess the statistical significance of the differences.

Cell Viability Test: Cytotoxicity was evaluated by MTS (3-(4,5-dimethylthiazol-2-yl)-5-(3-carboxymethoxyphenyl)-2-(4-sulfophenyl)-2H-tetrazolium) assay. Briefly, HeLa cells were seeded into a 96-well flat-bottom microtiter plate (3000 cells per well), incubated overnight, and then treated with GPMVs, copolymer-supplemented GPMVs, cross-linked-copolymer GPMVs, and various concentrations of copolymer for 24 h. The medium was then discarded and replaced with fresh medium (100 µL per well). MTS reagent (20 µL per well) was added to each well and incubated at 37 °C for 2 h. Next, the absorbance was measured at 490 nm and the background signal of the wells without cells was subtracted. Cell viability was calculated as the ratio of the absorbance of the sample-treated wells to that of the control wells (untreated) and expressed as a percentage. Tests were performed in quadruplicate. Each point represents the mean ± SD (bars) of replicates from one representative experiment.

pH-Triggered Dye Permeation at pH 6.0: The pH value of GPMVs, copolymer-supplemented GPMVs, and cross-linked-copolymer GPMVs dispersions was first adjusted down to 6.0 with HCl (0.5 M) and then the samples were left for 1 h to reach the equilibrium. Afterward, a solution of Alexa Fluor-633-NHS-ester (final concentration: 0.05 mg mL^{-1}) was added into all GPMVs samples with pH 6.0 and, after 1 h of incubation, the GPMVs were washed five times with GPMV buffer and the CLSM images were recorded.

pH-Induced Dye Release at pH 6.5: The cross-linked-copolymer GPMVs loaded with Atto-633 were prepared according to the method mentioned above for the dye leakage assay. The pH values of all samples were adjusted down to 6.5 with HCl (0.5 M) and the CLSM imaging of GPMVs was performed after 1 h of incubation.

All permeation and releasing experiments were conducted at room temperature. The mean fluorescence intensities were applied with the same method as given above in "Dye Permeation Study" section.

Antibody Staining: Cells: Cells were plated on 8-well chamber glass slide (IBIDI) in a density of 75 000 cells per well (MDA-MB-468) and 50 000 cells per well (HepG2). The plate was incubated for 48 h, then the culture medium was discarded, the cells were washed three times with PBS and fixed with 4% paraformaldehyde for 15 min. Cells were washed three times with PBS, blocked with 3% BSA in PBS for 1 h and stained with Hoechst 33342 at a concentration of 0.25 µg mL^{-1} for 20 min. Cells were washed again three times with PBS, and cell membranes were stained with WGA-Alexa Fluor 555 conjugate at a concentration of 5 µg mL^{-1} for 5 min in PBS at room temperature. Cells were washed three times with PBS and incubated overnight at 4 °C with mouse monoclonal antibody anti-EGFR diluted 1:100 in PBS with 3% BSA. Next day cells were washed with PBS and incubated for 2 h at room temperature with fluorescently labeled secondary antibody (Alexa Fluor 647 donkey anti-mouse IgG) diluted 1:200 in PBS with 3% BSA. Finally, cells were washed three times with PBS and imaged using CLSM.

GPMVs: GPMVs were placed in 8-well chamber glass slide (IBIDI) and incubated in PBS containing 3% BSA for 1 h at room temperature. Then GPMVs were incubated overnight at 4 °C with mouse monoclonal antibody anti-EGFR diluted 1:100 in PBS with 3% BSA. Next day GPMVs were washed with PBS and incubated for 2 h at room temperature with secondary antibody (Alexa Fluor 647 donkey anti-mouse IgG) diluted 1:200 in PBS with 3% BSA. Finally, GMPVs were washed three times with PBS and imaged using CLSM.

Supporting Information

Supporting Information is available from the Wiley Online Library or from the author.

Acknowledgements

The authors gratefully acknowledge the financial support provided by the Swiss National Science Foundation (SNSF), the National Centre of Competence in Research Molecular Systems Engineering, and the University of Basel. X.H. was supported by a China Scholarship Council (CSC), Grant No. 201808230256 Ph.D. fellowship. X.H. is grateful to Dr. M. Garni for advice on GPMVs modification methods, Dr. R. Wehr for GPC measurements and Dr. M. Kyropoulou, Dr. I. Craciun, Dr. P. Kong, and Dr. M. A. A. Garcia (University of Basel) for useful discussions. X.H. thanks Dr. O. Eggenberger for proofreading. X.H. thanks Dr. S. Li for the advice in analysis of the data and discussions. H.S. was supported by Grant No. 172824 of the Swiss National Science Foundation.

Conflict of Interest

The authors declare no conflict of interest.

Authors Contribution

Conceptualization: C.G.P.; Synthesis: X.H., D.W., I.A.D.; Investigation, methodology, and validation: X.H., D.H., H.S., M.S., and E.R.D.; Writing-review & editing: all co-authors.

Data Availability Statement

The data that support the findings of this study are available from the corresponding author upon reasonable request.

Keywords

cross-linking, giant plasma membrane vesicles, mechanical stability, membrane modification, pH-triggered permeability

Received: August 29, 2022
Published online: October 26, 2022

[1] H. Pick, A. C. Alves, H. Vogel, *Chem. Rev.* **2018**, *118*, 8598.

[2] S. Jeong, H. T. Nguyen, C. H. Kim, M. N. Ly, K. Shin, *Adv. Funct. Mater.* **2020**, *30*, 1907182.
[3] M. Garni, T. Einfalt, R. Goers, C. G. Palivan, W. Meier, *ACS Synth. Biol.* **2018**, *7*, 2116.
[4] S. Li, X. Wang, W. Mu, X. Han, *Anal. Chem.* **2019**, *91*, 6859.
[5] M. Morita, K. Katoh, N. Noda, *ChemistryOpen* **2018**, *7*, 845.
[6] A. Moga, N. Yandrapalli, R. Dimova, T. Robinson, *ChemBioChem* **2019**, *20*, 2674.
[7] S. Thamboo, A. Najer, A. Belluati, C. von Planta, D. Wu, I. Craciun, W. Meier, C. G. Palivan, *Adv. Funct. Mater.* **2019**, *29*, 1904267.
[8] A. Belluati, S. Thamboo, A. Najer, V. Maffeis, C. von Planta, I. Craciun, C. G. Palivan, W. Meier, *Adv. Funct. Mater.* **2020**, *30*, 2002949.
[9] E. Rideau, R. Dimova, P. Schwille, F. R. Wurm, K. Landfester, *Chem. Soc. Rev.* **2018**, *47*, 8572.
[10] Y. Lu, G. Allegri, J. Huskens, *Mater. Horiz.* **2022**, *9*, 892.
[11] S. I. Brett, Y. Kim, C. N. Biggs, J. L. Chin, H. S. Leong, *Prostate Cancer Prostatic Dis.* **2015**, *18*, 213.
[12] G. Raposo, W. Stoorvogel, *J. Cell Biol.* **2013**, *200*, 373.
[13] T. Baumgart, A. T. Hammond, P. Sengupta, S. T. Hess, D. A. Holowka, B. A. Baird, W. W. Webb, *Proc. Natl. Acad. Sci. USA* **2007**, *104*, 3165.
[14] R. Kalluri, V. S. LeBleu, *Science* **2020**, *367*, 6977.
[15] S. Son, S. C. Takatori, B. Belardi, M. Podolski, M. H. Bakalar, D. A. Fletcher, *Proc. Natl. Acad. Sci. USA* **2020**, *117*, 14209.
[16] J. B. Larsen, N. Taebnia, A. Dolatshahi-Pirouz, A. Z. Eriksen, C. Hjørringgaard, K. Kristensen, N. W. Larsen, N. B. Larsen, R. Marie, A.-K. Mündler, L. Parhamifar, A. J. Urquhart, A. Weller, K. I. Mortensen, H. Flyvbjerg, T. L. Andresen, *RSC Chem. Biol.* **2021**, *2*, 1115.
[17] S. García-Silva, M. Gallardo, H. Peinado, *Front. Cell Dev. Biol.* **2021**, *8*, 1820.
[18] E. M. Veziroglu, G. I. Mias, *Front. Genet.* **2020**, *11*, 700.
[19] B. Pang, Y. Zhu, J. Ni, J. Thompson, D. Malouf, J. Bucci, P. Graham, Y. Li, *Theranostics* **2020**, *10*, 2309.
[20] X. Jin, Y. Chen, H. Chen, S. Fei, D. Chen, X. Cai, L. Liu, B. Lin, H. Su, L. Zhao, M. Su, H. Pan, L. Shen, D. Xie, C. Xie, *Clin. Cancer Res.* **2017**, *23*, 5311.
[21] C. Eichelser, I. Stückrath, V. Müller, K. Milde-Langosch, H. Wikman, K. Pantel, H. Schwarzenbach, *OncoTargets Ther.* **2014**, *5*, 9650.
[22] L. Dong, W. Lin, P. Qi, M. Xu, X. Wu, S. Ni, D. Huang, W. Weng, C. Tan, W. Sheng, X. Zhou, X. Du, *Cancer Epidemiol. Biomarkers Prev.* **2016**, *25*, 1158.
[23] D. D. Taylor, C. Gercel-Taylor, *Gynecol. Oncol.* **2008**, *110*, 13.
[24] W. Zhou, X. Chen, Y. Zhou, S. Shi, C. Liang, X. Yu, H. Chen, Q. Guo, Y. Zhang, P. Liu, C. Li, Y. Chu, Y. Luo, Y. Wang, Z. Zhou, Z. Zhao, Q. Chen, T. Sun, C. Jiang, *Biomaterials* **2022**, *280*, 121306.
[25] R. C. de Abreu, C. V. Ramos, C. Becher, M. Lino, C. Jesus, P. A. da Costa Martins, P. A. T. Martins, M. J. Moreno, H. Fernandes, L. Ferreira, *J. Extracell. Vesicles* **2021**, *10*, 12111.
[26] H. Zhang, Y. Wang, M. Bai, J. Wang, K. Zhu, R. Liu, S. Ge, J. Li, T. Ning, T. Deng, Q. Fan, H. Li, W. Sun, G. Ying, Y. Ba, *Cancer Sci.* **2018**, *109*, 629.
[27] T. R. Lunavat, S. C. Jang, L. Nilsson, H. T. Park, G. Repiska, C. Lässer, J. A. Nilsson, Y. S. Gho, J. Lötvall, *Biomaterials* **2016**, *102*, 231.
[28] B. Escudier, T. Dorval, N. Chaput, F. André, M.-P. Caby, S. Novault, C. Flament, C. Leboulaire, C. Borg, S. Amigorena, C. Boccaccio, C. Bonnerot, O. Dhellin, M. Movassagh, S. Piperno, C. Robert, V. Serra, N. Valente, J.-B. L. Pecq, A. Spatz, O. Lantz, T. Tursz, E. Angevin, L. Zitvogel, *J. Transl. Med.* **2005**, *3*, 10.
[29] M. A. Morse, J. Garst, T. Osada, S. Khan, A. Hobeika, T. M. Clay, N. Valente, R. Shreeniwas, M. A. Sutton, A. Delcayre, D.-H. Hsu, J.-B. L. Pecq, H. K. Lyerly, *J. Transl. Med.* **2005**, *3*, 9.
[30] R. Kanchanapally, S. K. Deshmukh, S. R. Chavva, N. Tyagi, S. K. Srivastava, G. K. Patel, A. P. Singh, S. Singh, *Int. J. Nanomed.* **2019**, *14*, 531.
[31] Y. Hong, G.-H. Nam, E. Koh, S. Jeon, G. B. Kim, C. Jeong, D.-H. Kim, Y. Yang, I.-S. Kim, *Adv. Funct. Mater.* **2018**, *28*, 1703074.
[32] M. S. Kim, M. J. Haney, Y. Zhao, V. Mahajan, I. Deygen, N. L. Klyachko, E. Inskoe, A. Piroyan, M. Sokolsky, O. Okolie, S. D. Hingtgen, A. V. Kabanov, E. V. Batrakova, *Nanomedicine* **2016**, *12*, 655.
[33] S. Gurunathan, M.-H. Kang, M. Jeyaraj, M. Qasim, J.-H. Kim, *Cells* **2019**, *8*, 307.
[34] M. Li, L. Huang, J. Chen, F. Ni, Y. Zhang, F. Liu, *ACS Appl. Nano Mater.* **2021**, *4*, 3351.
[35] A. Jeyaram, S. M. Jay, *AAPS J.* **2017**, *20*, 1.
[36] F. Yuan, Y.-M. Li, Z. Wang, *Drug Delivery* **2021**, *28*, 1501.
[37] M. Richter, K. Fuhrmann, G. Fuhrmann, *J. Vis. Exp.* **2019**, *147*, e59584.
[38] S. Lathwal, S. S. Yerneni, S. Boye, U. L. Muza, S. Takahashi, N. Sugimoto, A. Lederer, S. R. Das, P. G. Campbell, K. Matyjaszewski, *Proc. Natl. Acad. Sci. USA* **2021**, *118*, e2020241118.
[39] E. Sezgin, H.-J. Kaiser, T. Baumgart, P. Schwille, K. Simons, I. Levental, *Nat. Protoc.* **2012**, *7*, 1042.
[40] I. Levental, K. R. Levental, F. A. Heberle, *Trends Cell Biol.* **2020**, *30*, 341.
[41] N. Del Piccolo, J. Placone, L. He, S. C. Agudelo, K. Hristova, *Anal. Chem.* **2012**, *84*, 8650.
[42] Š. Z. Jokhadar, U. Klančnik, M. Grundner, T. Švelc Kebe, S. V. Hartman, M. Lović, J. Derganc, *BMC Biophys.* **2018**, *11*, 1.
[43] I. Levental, M. Grzybek, K. Simons, *Proc. Natl. Acad. Sci. USA* **2011**, *108*, 11411.
[44] T. W. Han, W. Ye, N. P. Bethel, M. Zubia, A. Kim, K. H. Li, A. L. Burlingame, M. Grabe, Y. N. Jan, L. Y. Jan, *Proc. Natl. Acad. Sci. USA* **2019**, *116*, 1309.
[45] C. V. Kelly, M.-M. T. Kober, P. Kinnunen, D. A. Reis, B. G. Orr, M. M. Banaszak Holl, *J. Biol. Phys.* **2009**, *35*, 279.
[46] K. R. Levental, I. Levental, in *Current Topics in Membranes*, Vol. 75 (Ed: A. K. Kenworthy), Academic Press, Waltham, MA, USA **2015**, Ch. 2, pp. 25–57.
[47] A. Dubavik, E. Sezgin, V. Lesnyak, N. Gaponik, P. Schwille, A. Eychmüller, *ACS Nano* **2012**, *6*, 2150.
[48] S.-T. Yang, A. J. B. Kreutzberger, V. Kiessling, B. K. Ganser-Pornillos, J. M. White, L. K. Tamm, *Sci. Adv.* **2017**, *3*, 1700338.
[49] T. Einfalt, M. Garni, D. Witzigmann, S. Sieber, N. Baltisberger, J. Huwyler, W. Meier, C. G. Palivan, *Adv. Sci.* **2020**, *7*, 1901923.
[50] T. Togo, in *Current Topics in Membranes, Vol. 84* (Ed: L. O. Andrade), Academic Press, Cambridge, MA, USA **2019**, Ch. 5, pp. 99–127.
[51] Z.-J. Chen, S.-C. Yang, X.-L. Liu, Y. Gao, X. Dong, X. Lai, M.-H. Zhu, H.-Y. Feng, X.-D. Zhu, Q. Lu, M. Zhao, H.-Z. Chen, J. F. Lovell, C. Fang, *Nano Lett.* **2020**, *20*, 4177.
[52] J. I. Griffin, G. Wang, W. J. Smith, V. P. Vu, R. Scheinman, D. Stitch, R. Moldovan, S. M. Moghimi, D. Simberg, *ACS Nano* **2017**, *11*, 11584.
[53] S. Chatterjee, T. Ooya, *ACS Appl. Polym. Mater.* **2020**, *2*, 1909.
[54] K. Buyens, J. Demeester, S. S. De Smedt, N. N. Sanders, *Langmuir* **2009**, *25*, 4886.
[55] M. Mohamed, A. S. Abu Lila, T. Shimizu, E. Alaaeldin, A. Hussein, H. A. Sarhan, J. Szebeni, T. Ishida, *Sci. Technol. Adv. Mater.* **2019**, *20*, 710.
[56] L. Feng, M. Gao, D. Tao, Q. Chen, H. Wang, Z. Dong, M. Chen, Z. Liu, *Adv. Funct. Mater.* **2016**, *26*, 2207.
[57] X. Zhang, P. Angsantikul, M. Ying, J. Zhuang, Q. Zhang, X. Wei, Y. Jiang, Y. Zhang, D. Dehaini, M. Chen, Y. Chen, W. Gao, R. H. Fang, L. Zhang, *Angew. Chem., Int. Ed.* **2017**, *56*, 14075.
[58] H. Zhou, Z. Fan, P. K. Lemons, H. Cheng, *Theranostics* **2016**, *6*, 1012.
[59] L.-H. Peng, Y.-H. Zhang, L.-J. Han, C.-Z. Zhang, J.-H. Wu, X.-R. Wang, J.-Q. Gao, Z.-W. Mao, *ACS Appl. Mater. Interfaces* **2015**, *7*, 18628.

[60] S. Vogt, G. Stadlmayr, J. Grillari, F. Ruker, G. Wozniak-Knopp, in *Current Topics in Biochemical Engineering*, (Ed. N. Shiomi), IntechOpen, London, UK **2019**, Ch. 7, pp. 1–21.
[61] Y.-Y. Jhan, G. Palou Zuniga, K. A. Singh, A. K. Gaharwar, D. L. Alge, C. J. Bishop, *ACS Appl. Bio Mater.* **2021**, *4*, 1294.
[62] Y.-T. Chiang, Y.-T. Cheng, C.-Y. Lu, Y.-W. Yen, L.-Y. Yu, K.-S. Yu, S.-Y. Lyu, C.-Y. Yang, C.-L. Lo, *Chem. Mater.* **2013**, *25*, 4364.
[63] Y.-T. Chiang, S.-Y. Lyu, Y.-H. Wen, C.-L. Lo, *Int. J. Mol. Sci.* **2018**, *19*, 1615.
[64] D. Yang, D. F. O'Brien, S. R. Marder, *J. Am. Chem. Soc.* **2002**, *124*, 13388.
[65] S. Tang, K. Chi, H. Xu, Q. Yong, J. Yang, J. M. Catchmark, *Carbohydr. Polym.* **2021**, *252*, 117123.
[66] X. Chen, X. Zhang, H.-Y. Wang, Z. Chen, F.-G. Wu, *Langmuir* **2016**, *32*, 10126.
[67] Y. Li, H. Cong, S. Wang, B. Yu, Y. Shen, *Biomater. Sci.* **2020**, *8*, 6442.
[68] M. P. Robin, M. W. Jones, D. M. Haddleton, R. K. O'Reilly, *ACS Macro Lett.* **2012**, *1*, 222.
[69] E. Setijadi, L. Tao, J. Liu, Z. Jia, C. Boyer, T. P. Davis, *Biomacromolecules* **2009**, *10*, 2699.
[70] K. Shoji, Y. Nakajima, E. Ueda, M. Takeda, *Polym. J.* **1985**, *17*, 997.
[71] E. Gholizadeh, R. Belibel, T. Bachelart, C. Bounadji, C. Barbaud, *RSC Adv.* **2020**, *10*, 32602.
[72] Y. J. Ooi, Y. Wen, J. Zhu, X. Song, J. Li, *Biomacromolecules* **2020**, *21*, 1136.
[73] I. Levental, F. J. Byfield, P. Chowdhury, F. Gai, T. Baumgart, P. A. Janmey, *Biochem. J.* **2009**, *424*, 163.
[74] K. Farsad, P. D. Camilli, *Curr. Opin. Cell Biol.* **2003**, *15*, 372.
[75] T. Itoh, T. Takenawa, *Prog. Lipid Res.* **2009**, *48*, 298.
[76] B. Alberts, A. Johnson, J. Lewis, M. Raff, K. Roberts, P. Walter, in *Molecular Biology of the Cell*, 4th ed., Garland Science, New York, NY, USA **2002**.
[77] L. Zartner, M. Garni, I. Craciun, T. Einfalt, C. G. Palivan, *Biomacromolecules* **2021**, *22*, 106.
[78] G. H. Leno, C. S. Downes, R. A. Laskey, *Cell* **1992**, *69*, 151.
[79] M. Nazari, M. Kurdi, H. Heerklotz, *Biophys. J.* **2012**, *102*, 498.
[80] J. S. Nanda, J. R. Lorsch, in *Methods in Enzymology*, Vol. 536 (Ed: J. Lorsch), Academic Press, San Diego, CA, USA **2014**, Ch. 8, pp. 87–94.
[81] A. Lorents, P. Säälik, Ü. Langel, M. Pooga, *Bioconjugate Chem.* **2018**, *29*, 1168.
[82] G. D. Kusuma, M. Barabadi, J. L. Tan, D. A. V. Morton, J. E. Frith, R. Lim, *Front. Pharmacol.* **2018**, *9*, 1199.
[83] S. Bosch, L. de Beaurepaire, M. Allard, M. Mosser, C. Heichette, D. Chrétien, D. Jegou, J.-M. Bach, *Sci. Rep.* **2016**, *6*, 36162.
[84] J. Steinkühler, E. Sezgin, I. Urbančič, C. Eggeling, R. Dimova, *Commun. Biol.* **2019**, *2*, 337.
[85] D. A. Los, N. Murata, *Biochim. Biophys. Acta* **2004**, *1666*, 142.
[86] H. T. Spanke, R. W. Style, C. François-Martin, M. Feofilova, M. Eisentraut, H. Kress, J. Agudo-Canalejo, E. R. Dufresne, *Phys. Rev. Lett.* **2020**, *125*, 198102.
[87] S. Ballweg, E. Sezgin, M. Doktorova, R. Covino, J. Reinhard, D. Wunnicke, I. Hänelt, I. Levental, G. Hummer, R. Ernst, *Nat. Commun.* **2020**, *11*, 756.
[88] P. Noutsi, E. Gratton, S. Chaieb, *PLoS One* **2016**, *11*, 0158313.
[89] W. Stillwell, in *An Introduction to Biological Membranes*, 2nd ed. (Ed: W. Stillwell), Elsevier, Amsterdam **2016**, pp. 135–108.
[90] L. Michalek, L. Barner, C. Barner-Kowollik, *Adv. Mater.* **2018**, *30*, 1706321.
[91] P. J. Flory, *J. Chem. Phys.* **1949**, *17*, 303.
[92] B. Zhao, W. J. Brittain, *Prog. Polym. Sci.* **2000**, *25*, 677.
[93] N. F. Steinmetz, M. Manchester, *Biomacromolecules* **2009**, *10*, 784.
[94] P. W. Fowler, J. Hélie, A. Duncan, M. Chavent, H. Koldsø, M. S. P. Sansom, *Soft Matter* **2016**, *12*, 7792.
[95] P. Shchelokovskyy, S. Tristram-Nagle, R. Dimova, *New J. Phys.* **2011**, *13*, 025004.
[96] R. Sorkin, R. Huisjes, F. Bošković, D. Vorselen, S. Pignatelli, Y. Ofir-Birin, J. K. F. Leal, J. Schiller, D. Mullick, W. H. Roos, G. Bosman, N. Regev-Rudzki, R. M. Schiffelers, G. J. L. Wuite, *Small* **2018**, *14*, 1801650.
[97] R. Dimova, *Adv. Colloid Interface Sci.* **2014**, *208*, 225.
[98] H. Bouvrais, L. Duelund, J. H. Ipsen, *Langmuir* **2014**, *30*, 13.
[99] J. Henriksen, A. C. Rowat, J. H. Ipsen, *Eur. Biophys. J.* **2004**, *33*, 732.
[100] H. Gurdal, M. M. Tuglu, S. Y. Bostanabad, B. Dalkiliç, *Int. J. Oncol.* **2019**, *54*, 1345.
[101] P. Zhao, X. Yang, S. Qi, H. Liu, H. Jiang, S. Hoppmann, Q. Cao, M.-S. Chua, S. K. So, Z. Cheng, *Biomed. Res. Int.* **2013**, *2013*, 759057.